8-11-1958

A Transient Thermal Analog of Nuclear Reactors

James R. Hume

A TRANSIENT THERMAL ANALOG OF NUCLEAR REACTORS - HUME

A TRANSIENT THERMAL ANALOG OF NUCLEAR REACTORS

By

James R. Hume

A Thesis

Submitted in Partial Fulfillment of the

Requirements for the Degree of

Master of Science in Engineering

The University of New Mexico

1958

This thesis, directed and approved by the candidate's committee, has been accepted by the Graduate Committee of the University of New Mexico in partial fulfillment of the requirements for the degree of

MASTER OF SCIENCE

E. P. Castetter
DEAN

August 11, 1958
DATE

Thesis committee

Victor J. Skoglund
CHAIRMAN

R. D. Ford

Edward C. Rightley

TABLE OF CONTENTS

LIST OF NOMENCLATURE

x = distance in direction of coolant flow

t = time

U_g = steady power, BTU/hr

ΔU_g = step increase in power, BTU/hr

h = heat transfer coefficient, BTU/f^2 hr ^oF

p = perimeter of fuel element, f

m = fuel element temperature, ^oF

f = bulk coolant temperature, ^oF

c = specific heat, BTU/lb ^oF

γ = specific weight, lb/f^3

A = cross-sectional area, f^2

w = fluid flow rate, lb/hr

X = similarity number, non-dimensional distance

T = similarity number, non-dimensional time

M = similarity number, non-dimensional metal temperature

F = similarity number, non-dimensional fluid temperature

a = similarity number, ratio of heat capacities

$b = 1 + 1/a$

$\bar{F} = \bar{F}(X,p)$, where p is complex Laplace variable

$\bar{M} = \bar{M}(X,p)$, where p is complex Laplace variable

V = fluid velocity, f/hr

z = variable of integration

D = inside diameter of circular coolant flow channel, effective diameter of annular coolant flow channel, f

k = thermal conductivity, BTU/f hr ^{o}F

G = mass velocity = w/A

μ = dynamic viscosity, lb hr/f^2

K = conversion factor for galvanometer trace deflection, ^{o}F/in

W = weight of thermocouple

Subscripts m and f refer to metal and fluid properties.

LIST OF TABLES

LIST OF FIGURES

ACKNOWLEDGEMENTS

The author is grateful for the assistance and encouragement received during the course of this investigation. Appreciation is expressed to Dr. V. J. Skoglund, thesis adviser; Dr. Robert Fannin for valuable suggestions in connection with the analytical solutions; and Mr. Thomas Summers for the development of a low-level current amplifier for use with thermocouples.

Invaluable services were performed by the author's wife, Mary L. Hume, who provided continual encouragement and performed a difficult job of typing to make this paper possible.

JRH

CHAPTER 1

INTRODUCTION

The nuclear reactor is presently receiving considerable attention as a possible source of energy for stationary power plants and propulsion systems. This has stimulated interest in many engineering problems which become very significant in reactor design work. The response of the reactor core heat transfer system to changes in power generation is one of these problems.

In the reactor, steady power level operation is achieved when the chain reaction is just self-sustaining, i.e. the reproduction of neutrons is exactly one. The expression "reactivity" is defined as the percentage by which the actual reproduction of neutrons differs from one. Positive changes in reactivity can result from many factors such as removal of neutron poisons, insertions of fissioning, moderating, or reflecting materials, and as a result of local temperature changes. Changes such as these occur from start-up and shut-down procedures, changing power demands, and accidents. The effect of positive reactivity is to put the reactor on an approximate exponential power rise which continues until the excess reactivity is removed by some means. Under certain conditions the rate of power increase may be quite high, hence the nuclear reactor has the potential for very large and rapid thermodynamic transients.

Knowledge of the transient response of the reactor core heat transfer system is important design information for control system specification, determination of maximum operating

temperatures, analysis of thermal stresses, and complete nuclear analysis.

The typical gas-cooled reactor consists of a large mass of neutron moderating material perforated by channels which extend through the assembly. Centered in the channels are the fuel elements. The coolant gas, which is usually pressurized, flows in the channel between fuel and moderator. It is usual to assume that 90% of the heat produced appears in the fuel and 10% in the moderator. The intensity of heat generation is a function of position in the reactor and may be described by trigonometric or Bessel functions depending on the core geometry.

THE INVESTIGATION

The problem of this investigation is the transient response of the bulk coolant temperature and the fuel temperature of a nuclear reactor as a result of a power excursion. The problem is attacked both theoretically and experimentally.

The theoretical portion includes a similarity analysis of an idealized mathematical model of the fuel and coolant channel. This analysis leads to non-dimensional differential equations for which an analytical solution was obtained. Because this solution is so complex, the numerical solution of another investigator is used for comparison with measurements.

The experimental investigations result in measured temperatures produced by a thermal analog of a reactor fuel and coolant channel. The time variation of the metal temperature was

determined at several positions on the model and coolant temperature was determined at the outlet end. Parameters varied were the rate of heat generation and the coolant flow rate.

The measured temperatures were converted to non-dimensional terms so that a comparison could be made between the experimental and theoretical results. A cross-plot of experimental data was made to show the consistency of data and to demonstrate the significance of the similarity numbers.

CHAPTER 2

LITERATURE REVIEW

Analysis of the complete nuclear reactor response to transient changes in reactivity has been presented by several authors in the unclassified literature. Notable among these is Schultz(1)[+] who lumps spacial effects and makes other simplifying assumptions that permit him to express heat transfer phenomenon in the form of "transfer functions." These are combined with the transfer functions of other reactor processes associated with the transient to give a prediction of the response of the entire nuclear system. This technique omits details of the heat transfer transient to permit solution of the larger problem. A more complex treatment is presented by Howard(2) who considers in some detail the average cell in a heterogeneous reactor. Although the heat transfer process is given considerable attention, spacial variations are averaged to permit more emphasis to be placed on the "neutronics" of the problem.

Exclusive attention is given to the thermodynamic aspects of reactor transients in the paper by Brown(3) who emphasized that the transient analysis must be based on the generalized

---

[+]Numbers in parentheses refer to the LIST OF REFERENCES in the Appendix.

laws of thermodynamics rather than on a succession of steady state equations. An approximate method for predicting the rise of reactor temperatures following start-up is presented in an article by Bonilla(4). His solution is achieved by numerical solution of finite steps in space and time.

Hellman, Habetler, and Barbrov(5) have set up the thermal transient problem for the whole core of a liquid metal-cooled reactor in the form of a thermal network for numerical solution. Heat generation and transmission are considered as functions of time and two space variables. Temperatures and thermal properties are space and time averaged for each space and time node. This leads to more than 110 finite difference equations and solution was accomplished on a high-speed digital computer. The application of numerical methods to transient problems involving a perturbation in initial coolant temperature or direction of coolant flow has been presented by Dusinberre(6).

Paynter and Takahashi(7) have published a method for computing the response of heat exchangers from an analogy between their equations and those from statistics. The response of a fluid flowing through an insulated pipe subject to a step increase in the inlet temperature has been published by Rizika(8,9) for both compressible and incompressible flow.

By far the most pertinent work is that of Clark, Arpaci, and Treadwell(10,11) which appeared while this investigation was in progress. These authors had derived differential

equations by a similar method and with the same assumptions as those presented in this thesis. Their solutions were also obtained by use of the Laplace transform and are similar. Improvement in the form of the solutions results from the use of non-dimensional equations here and from the use of alternate mathematical methods of inversion. The experimental verification exhibited with the papers by Clark, et al, was contributed by Treadwell(12) and Stuart(13) in their thesis work at Massachusetts Institute of Technology. Their experiments were performed on equipment nearly identical to that used in this investigation and included the measurement of fluid and metal temperatures at two locations for temperature changes on the order of 50°F. Their coolant fluid was water whereas air was used here.

Numerical solutions to the non-dimensional differential equations were calculated by Bankston(14) in connection with this project.

CHAPTER 3

THEORETICAL INVESTIGATION

A physical system typical of this problem may be described as a solid cylindrical metal fuel rod within a concentric circular channel through the moderating material. The annular space is filled with pressurized gas which flows in the positive x direction. The transient increase in power occurs at time $t = 0$. A cross-section of a differential element is shown in Figure 1.

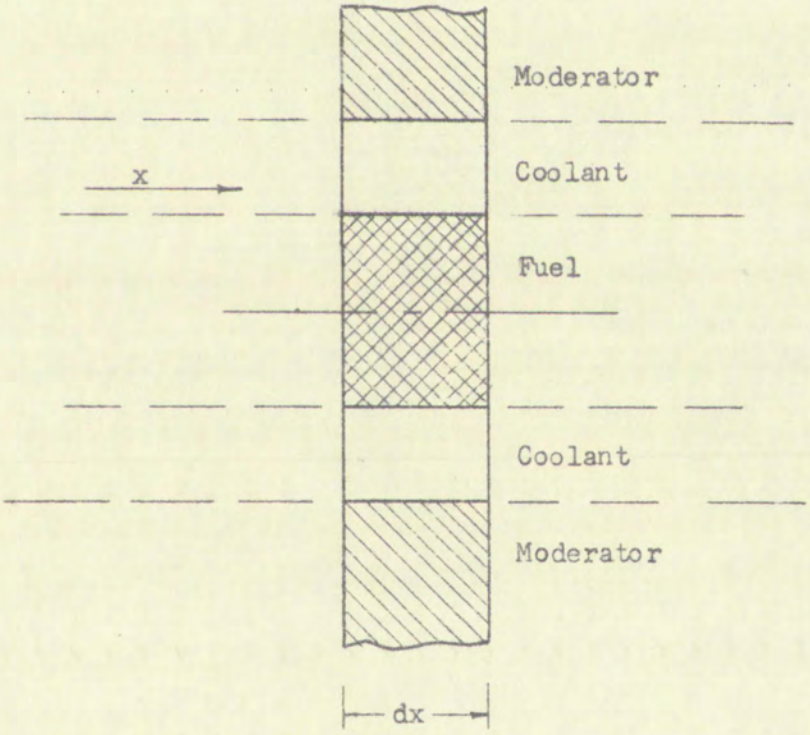

Figure 1 Differential Cross-section of a Fuel Element and Its Cooling Channel

The theoretical problem is simplified by the following assumptions:

1. The interface between moderator and coolant is adiabatic.
2. There is a stepwise increase in power with respect to time.
3. There are no radial temperature gradients in either the metal or the fluid, but there is convection heat transfer from the fuel to the gas.
4. There is no axial heat conduction.
5. All metal and fluid properties are constant.
6. The heat transfer coefficient $h \neq f(x,t)$.

DERIVATION OF DIFFERENTIAL EQUATIONS

The differential section in Figure 1 may be regarded as two parts: the fluid part and the metal part. Each of these yields an energy balance equation. For the metal part

$$(U_g + \Delta U_g)dx = h\ p\ (m - f)\ dx + c_m \gamma_m A_m \left(\frac{\partial m}{\partial t}\right) dx \qquad 1$$

and for the fluid part

$$h\ p\ (m - f) = w\ c_f\ df \qquad 2$$

where U_g = steady power, BTU/hr

ΔU_g = step increase in power, BTU/hr

h = heat transfer coefficient, BTU/f^2hr^oF

p = perimeter of fuel element, f

m = metal temperature, ^{o}F

f = fluid temperature, ^{o}F

c = specific heat (at constant pressure for the fluid), BTU/lb^{o}F

γ = specific weight, lb/f^3

A = cross-sectional area in radial plane, f^2

w = fluid flow rate, lb/hr

and the subscripts m and f refer to the metal and fluid parts. Since f = f(x,t), then

$$df = \frac{\partial f}{\partial x}\,dx + \frac{\partial f}{\partial t}\,dt.$$

Also $w = \gamma_f A_f V$ where V is the fluid velocity.

Equations 1 and 2 may be rearranged to form

$$(m - f) = \frac{U_g + \Delta U_g}{hp} - \frac{c_m \gamma_m A_m}{hp}\left(\frac{\partial m}{\partial t}\right)$$

$$= \frac{U_g + \Delta U_g}{hp} - \frac{c_m \gamma_m A_m}{hp}\left(\frac{\partial m}{\partial t}\right) \qquad 3$$

and

$$(m - f) = \frac{w\, c_f}{hp}\left(\frac{\partial f}{\partial x}\right) + \frac{c_f \gamma_f A_f}{hp}\left(\frac{\partial f}{\partial t}\right). \qquad 4$$

The steady and transient parts of equations 3 and 4 may be separated by the substitution

$$m = m' + m'' \text{ and } f = f' + f''$$

where the single prime denotes the steady state temperature for $t < 0$ when $\frac{\partial m'}{\partial t} = \frac{\partial f'}{\partial t} = 0$, and the double prime denotes the

transient part. Then

$$m' - f' + m'' - f'' = \frac{U_g}{hp} + \frac{\Delta U_g}{hp} - \frac{c_m \gamma_m A_m}{hp} \left(\frac{\partial m''}{\partial t}\right) \qquad 5$$

and

$$m' - f' + m'' - f'' = \frac{w\, c_f}{hp} \left(\frac{\partial f'}{\partial x} + \frac{\partial f''}{\partial x}\right) + \frac{c_f \gamma_f A_f}{hp} \left(\frac{\partial f''}{\partial t}\right) \qquad 6$$

But when $t < 0$, $m' - f' = \frac{U_g}{hp}$ 7

$$m' - f' = w\, c_f \left(\frac{\partial f'}{\partial x}\right). \qquad 8$$

By combining equations 5, 6, 7, and 8, the differential equations for $t \geq 0$ become

$$m'' - f'' = \frac{\Delta U_g}{hp} - \frac{c_m \gamma_m A_m}{hp} \left(\frac{\partial m''}{\partial t}\right) \qquad 9$$

$$m'' - f'' = \frac{w\, c_f}{hp} \left(\frac{\partial f''}{\partial x}\right) + \frac{c_f \gamma_f A_f}{hp} \left(\frac{\partial f''}{\partial t}\right) \qquad 10$$

This illustrates that the transient parts of the temperatures are independent and may be superimposed upon the steady state temperature profiles. Henceforth, the double primes will be omitted but it will be recalled that temperatures refer only to the transient part.

DIMENSIONAL ANALYSIS

A further simplification results if equations 9 and 10 are converted to non-dimensional form. The number of similarity numbers is determined by the Buckingham Pi theorem. In this

problem the number of variables n = 9: (m), (f), (x), (t), ($w\,c_f$), ($c_f\,\gamma_f A_f$), ($c_m\,\gamma_m A_m$), (ΔU_g), and (hp). The number of primary independent units p = 4: (mass), (length), (time), and (temperature). Then the number of similarity numbers to be expected is n - p = 5. Since m and f of the original nine variables are dependent, then there should be 2 dependent and 3 independent similarity numbers.

An inspection of the differential equations 9 and 10 indicates that two of the independent similarity numbers are

$$X = \frac{xhp}{wc_f} \quad \text{and} \quad T = \frac{thp}{c_f\,\gamma_f A_f}$$

where X and T are non-dimensional lengths and time. The third independent similarity number appears later in the derivation. The two dependent similarity numbers are expressed initially as $m = K_m M$ and $f = K_f F$ where M and F are non-dimensional temperatures. Then

$$\left(\frac{\partial m}{\partial t}\right) = K_m\left(\frac{\partial M}{\partial T}\right)\left(\frac{\partial T}{\partial t}\right) = K_m\left(\frac{hp}{c_f\,\gamma_f A_f}\right)\left(\frac{\partial M}{\partial T}\right)$$

$$\left(\frac{\partial f}{\partial x}\right) = K_f\left(\frac{\partial F}{\partial X}\right)\left(\frac{\partial X}{\partial x}\right) = K_f\left(\frac{hp}{wc_f}\right)\left(\frac{\partial F}{\partial X}\right)$$

$$\left(\frac{\partial f}{\partial t}\right) = K_f\left(\frac{hp}{c_f\,\gamma_f A_f}\right)\left(\frac{\partial F}{\partial T}\right)$$

Substituting the above into 9 and 10 results in

$$K_m M - K_f F = \frac{\Delta U_g}{hp} - K_m\left(\frac{c_m\,\gamma_m A_m}{c_f\,\gamma_f A_f}\right)\left(\frac{\partial M}{\partial T}\right)$$

$$K_m M - K_f F = K_f\left(\frac{\partial F}{\partial T}\right) + K_f\left(\frac{\partial F}{\partial X}\right)$$

It is now apparent that the third similarity number ought to be $a = \frac{c_m \gamma_m A_m}{c_f \gamma_f A_f}$ and for the simplest form $K_m = K_f = \frac{\Delta U_g}{hp}$.

Now the differential equations to be solved are:

$$M - F = 1 - a\frac{\partial M}{\partial T} \qquad 11$$

$$M - F = \frac{\partial F}{\partial X} + \frac{\partial F}{\partial T} \qquad 12$$

where the similarity numbers are defined as $M \equiv \frac{mhp}{\Delta U_g}$, $F \equiv \frac{fhp}{\Delta U_g}$, $X \equiv \frac{xhp}{wc_f}$, $T \equiv \frac{thp}{c_f \gamma_f A_f}$, and $a \equiv \frac{c_m \gamma_m A_m}{c_f \gamma_f A_f}$.

In order to simulate variations in properties with temperature, it is necessary that $(\text{temperature})_A = (\text{temperature})_P$ where the subscripts A and P refer to analog and prototype respectively. The temperature criteria above indicates that this requirement can be met by assuring that

$$\frac{(\Delta U_g)_A}{(\Delta U_g)_P} = \frac{(hp)_A}{(hp)_P} .$$

Analog length and time scales are determined from the non-dimensional length and time criteria:

$$\frac{x_A}{x_P} = \frac{(wc_f)_A}{(wc_f)_P}\frac{(hp)_P}{(hp)_A} \qquad \text{and} \qquad \frac{t_A}{t_P} = \frac{(c_f \gamma_f A_f)(hp)_P}{(c_f \gamma_f A_f)(hp)_A} .$$

ANALYTICAL SOLUTION

Equations 11 and 12 may be solved explicity for M and F to obtain

$$\frac{\partial^2 F}{\partial T^2} + \frac{\partial^2 F}{\partial X T} + (1 + 1/a)\frac{\partial F}{\partial T} + (1/a)\frac{\partial F}{\partial X} - (1/a) = 0 \qquad 13$$

and

$$\frac{\partial^2 M}{\partial T^2} + \frac{\partial^2 M}{\partial X T} + (1 + 1/a)\frac{\partial M}{\partial T} + (1/a)\frac{\partial M}{\partial X} - (1/a) = 0 \qquad 14$$

Equations 13 and 14 may be operated on by the Laplace transform method in which the needed transformations are found in the references(15,16,17). The following transforms will be used:

$$L[1 - e^{-T/a}] = \frac{a}{p(p + 1/a)}$$

$$L[g(X,T)] = \int_0^\infty e^{-pt}[g(X,T)dT] = \bar{g}(X,p)$$

$$L[\frac{\partial^2 g}{\partial T^2}] = p^2\bar{g} - p[g(X,+0)] - \frac{\partial g}{\partial T}(X,+0)$$

$$L[\frac{\partial^2 g}{\partial X \partial T}] = \frac{\partial}{\partial X}[p\bar{g} - g(X,+0)]$$

$$L[\frac{\partial g}{\partial T}] = p\bar{g} - g(X,+0)$$

$$L[\frac{\partial g}{\partial X}] = \frac{\partial \bar{g}}{\partial X}$$

$$L[1/a] = 1/ap$$

The initial conditions imposed on this problem are:

a. $F(X,+0) = 0$

b. $\frac{\partial F}{\partial T}(X,+0) = 0$

c. $M(X,+0) = 0$

d. $\frac{\partial M}{\partial T}(X,+0) = 1/a$

Hence the transformed equation 13 is

$$p^2\bar{F} + \frac{\partial}{\partial X}(p\bar{F}) + (1 + 1/a)p\bar{F} + (1/a)\frac{\partial \bar{F}}{\partial X} - 1/ap = 0$$

or

$$\frac{\partial \bar{F}}{\partial X} + \frac{p^2 + p + p/a}{p + 1/a}\bar{F} = \frac{1/a}{p(p + 1/a)} \qquad 15$$

and the transformed equation 14 is

$$p^2\bar{M} - 1/a + \frac{\partial}{\partial X}(p\bar{M}) + (1 + 1/a)p\bar{M} + (1/a)\frac{\partial \bar{M}}{\partial X} - 1/ap = 0$$

or

$$\frac{\partial \bar{M}}{\partial X} + \frac{p^2 + p + p/a}{p + 1/a}\bar{M} = \frac{1/a(p + 1)}{p(p + 1/a)}. \qquad 16$$

Equations 15 and 16 may be readily solved as ordinary differential equations. The boundary condition, $F(T,0) = 0$, $\bar{F}(p,0) = 0$, provides for the transformed solution of equation 15:

$$\bar{F}(X,p) = \frac{1/a}{p^2(p + 1 + 1/a)}\left[1 - \exp - \frac{p(p + 1 + 1/a)X}{(p + 1/a)}\right]. \qquad 17$$

A suitable boundary condition for equation 16 may be obtained from equation 11 where $F(0,T) = 0$ so that

$$\frac{\partial M}{\partial T}(0,T) + (1/a)\, M(0,T) = 1/a.$$

Operating on this by the Laplace transform yields

$$p\bar{M}(0,p) - M(0,+0) + (1/a)\bar{M}(0,p) = (1/ap) \text{ or } \bar{M}(0,p) = \frac{1/a}{p(p + 1/a)}$$

since $M(X,+0) = 0$. Then the transformed solution for equation 16 is

$$\bar{M}(X,p) = \frac{1/a(p + 1)}{p^2(p + 1 + 1/a)}$$

$$- \left[\frac{1/a^2}{p^2(p + 1 + 1/a)(p + 1/a)}\right]\exp - \frac{p(p + 1 + 1/a)}{p + 1/a}X. \qquad 18$$

The inversion of equations 17 and 18 is simplified by expanding the first fractions in each into partial fractions and by performing the division in the exponential. It is convenient to let $b \equiv 1 + 1/a$. Then

$$\bar{F}(X,p) = - \frac{1}{ab^2p} + \frac{1}{abp^2} + \frac{1}{ab^2(p + b)}$$

$$- \frac{1}{ap^2(p + b)}\left[\exp - pX - X + \frac{X/a}{p + 1/a}\right] \qquad 19$$

and

$$\bar{M}(X,p) = \frac{1}{a^2b^2p} + \frac{1}{abp^2} - \frac{1}{a^2b^2(p + b)}$$

$$- \frac{1/a^2}{p^2(p + b)(p + 1/a)}\left[\exp - pX - X + \frac{X/a}{p + 1/a}\right] \qquad 20$$

Difficulty arises in obtaining the inverse solution because of the term $\exp \frac{X/a}{p + 1/a}$. However, this may be expanded into the power series $1 + \frac{(X/a)(p + 1/a)^{-1}}{1!} + \frac{(X/a)^2(p + 1/a)^{-2}}{2!} + \ldots$

$$+ \frac{(X/a)^n(p + 1/a)^{-n}}{n!} \qquad n = 1, 2, 3, \ldots$$

An alternate approach to this difficulty is to arrange terms involving p such that the inverse is one of the Bessel functions(10,11). However, difficulty arises later when performing

the integration in the convolution method. Some assistance might be provided here by referring to the work by Wheelon and Robacker(18).

The terms in equation 19 and 20 must now be properly grouped.

$$\bar{F}(X,p) = -\frac{1}{ab^2p} + \frac{1}{ab\,p^2} + \frac{1}{ab^2(p+b)}$$

$$- \frac{e^{-X}}{a}\left[\left(\frac{e^{-pX}}{p^2}\right)\left(\frac{1}{p+b}\right)\right]$$

$$- \frac{e^{-X}}{a}\left[\left(\frac{e^{-pX}}{p^2}\right)\left(\frac{1}{p+b}\right)\sum_{1}^{\infty}\frac{(X/a)^n(p+1/a)^{-n}}{n!}\right] \qquad 21$$

$$\bar{M}(X,p) = \frac{1}{a^2b^2p} + \frac{1}{abp^2} - \frac{1}{a^2b^2(p+b)}$$

$$- \frac{e^{-X}}{a}\left[\left(\frac{e^{-pX}}{p^2}\right)\left(\frac{1}{p+b}\right)\left(\frac{1}{p+1/a}\right)\right]$$

$$- \frac{e^{-X}}{a}\left[\left(\frac{e^{-pX}}{p^2}\right)\left(\frac{1}{p+b}\right)\left(\frac{1}{p+1/a}\right)\sum_{1}^{\infty}\frac{(X/a)^n(p+1/a)^{-n}}{n!}\right] \qquad 22$$

The inverse functions required are as follows:

		Restrictions
$L^{-1}[(p+1/a)^{-n}]$	$= \frac{T^{n-1}e^{-T/a}}{(n-1)!}$	$T>0$
$L^{-1}[1/p]$	$= 1$	$T>0$
$L^{-1}[1/p^2]$	$= T$	$T>0$
$L^{-1}\left[\frac{1}{p+b}\right]$	$= e^{-bT}$	$T>0$
$L^{-1}\left[\frac{1}{p+1/a}\right]$	$= e^{-T/a}$	$T>0$
$L^{-1}\left[\frac{e^{-pX}}{p^2}\right]$	$= 0$ $= T - X$	$0<T<X$ $T>X$

The restrictions on the term (T - X) implies that the inverse solutions must be handled separately for each of two time intervals: $0 \leqq T \leqq X$ and $T > X$. Referring to the definitions, $T > X$ is equivalent to $t > x/V$ where V is the fluid velocity. This has the physical significance that until $t = x/V$ no fresh fluid has reached point x and the temperatures are independent of x. After $t = x/V$, fluid which was not in the channel at $t = 0$ influences temperatures at x and the temperatures are dependent on x.

The solutions of 19 and 20 for the first time interval are

$$F(X,T) = T/ab + 1/ab^2[e^{-bT} - 1] \qquad 23$$

and

$$M(X,T) = T/ab - 1/a^2b^2[e^{-bT} - 1]. \qquad 24$$

The solutions for the second time interval, $T > X$, are

$$F(X,T) = T/ab + 1/ab^2[e^{-bT} - 1] - \frac{e^{-X}}{a}[T - X)*(e^{-bT})] - \frac{e^{-X}}{a}[T - X)*(e^{-bT})*\sum_{1}^{\infty}\frac{(X/a)^n\ T^{n-1}\ e^{-T/a}}{n!\ (n-1)!}] \qquad 25$$

and

$$M(X,T) = T/ab - 1/a^2b^2[e^{-bT} - 1] - \frac{e^{-X}}{a^2}[(T - X)*(e^{-bT})*(e^{-T/a})] - \frac{e^{-X}}{a^2}[(T - X)*(e^{-bT})*(e^{-T/a})*\sum_{1}^{\infty}\frac{(X/a)^n\ T^{n-1}\ e^{-T/a}}{n!\ (n-1)!}] \qquad 26$$

where the asterisks indicate that the terms so connected are to be treated by the method of convolution. This is a technique for the inverse transformation for the product of functions and is discussed by Churchill(16), pages 36-40 and by Pipes(17), pages 525-526. The following equations illustrate the general convolution technique:

$$\bar{g}_1(X,p)\ \bar{g}_2(X,p) = g_1(X,T)*g_2(X,T)$$

$$g_1(X,T)*g_2(X,T) = \int_0^T g_1(X,T-z)\ g_2(X,z)\ dz$$

$$= \int_0^X g_1(X,T-z)\ g_2(X,z)\ dz$$

$$+ \int_X^T g_1(X,T-z)\ g_2(X,z)\ dz$$

In this problem, the inverse transformation of $\frac{e^{-pX}}{p^2}$ is involved in all the convolution operations. When $T < X$ the inverse is zero and therefore the integral from 0 to X is zero. Equations 25 and 26 are restricted in application to $T > X$ and the convolution integral has the limits X to T.

The convolutions required for equations 25 and 26 are now performed.

In equation 25

$$(T-X)*(e^{-bT}) = \int_X^T (T-z-X)e^{-bz}dz$$

$$= (T-X)\int_X^T e^{-bz}dz - \int_X^T ze^{-bz}dz$$

$$= \frac{T}{b} e^{-bX} + [\frac{X}{b} + \frac{1}{b^2}]e^{-bT} - [\frac{2X}{b} + \frac{1}{b^2}]e^{-bX}$$

$$= \frac{T}{b} e^{-bX} + Ae^{-bT} - B$$

In equation 26

$$(T - X)*(e^{-bT})*(e^{-T/a}) = \int_X^T e^{-(T - z)/a}\left[\frac{z}{b} e^{-bX} + Ae^{-bz} - B\right] dz$$

$$= e^{-T/a}\left[\frac{e^{-bX}}{b} \int_X^T ze^{z/a}dz + A \int_X^T e^{-z}dz\right.$$

$$\left. - B\int_X^T e^{z/a}dz\right]$$

$$= (aT - a^2)\frac{e^{-bX}}{b} - (Xa - a^2)\frac{e^{-X}e^{-T/a}}{b}$$

$$- Ae^{-bT} + Ae^{-X}e^{-T/a} - aB + aB\, e^{X/a}e^{-T/a}$$

$$= \frac{aT}{b} e^{-bX} - Ae^{-bT} - (aB + \frac{a^2}{b} e^{-bX})$$

$$+ \left[(Ab - aX + a^2)\frac{e^{-X}}{b} + aB\, e^{X/a}\right] e^{-T/a}$$

$$= \frac{aT}{b} e^{-bX} - Ae^{-bT} - C + De^{-T/a}$$

In equation 25

$$(\frac{T}{b} e^{-bX} + Ae^{-bT} - B)* \sum_1^{\infty} \frac{(X/a)^n\, T^{n-1}\, e^{-T/a}}{n!\ (n - 1)!} =$$

$$= \frac{e^{-bX}}{b} \sum_1^{\infty} \frac{(X/a)^n}{n!\ (n - 1)!} \int_X^T (T - z)z^{n-1}\, e^{-z/a}dz$$

$$+ A\sum_{1}^{\infty} \frac{(X/a)^n}{n!\,(n-1)!} \int_X^T e^{-b(T-z)} z^{n-1}\, e^{-z/a}\, dz$$

$$- B\sum_{1}^{\infty} \frac{(X/a)^n}{n!\,(n-1)!} \int_X^T z^{n-1}\, e^{-z/a}\, dz$$

Without evaluating integrals, this is of the form

$$= \frac{e^{-bx}}{b}\,\Sigma_1 + A\Sigma_2 - B\Sigma_3$$

where Σ_1, Σ_2 and Σ_3 involve combinations of series.
In equation 26

$$\left(\frac{aT}{b}\, e^{-bX} - Ae^{-bT} - C + De^{-T/a}\right) * \sum_{1}^{\infty} \frac{(X/a)^n\, T^{n-1}\, e^{-T/a}}{n!\,(n-1)!} =$$

$$= \frac{a}{b}\, e^{-bX}\,\Sigma_1 - A\Sigma_2 - C\Sigma_3$$

$$+ D\sum_{1}^{\infty} \frac{(X/a)}{n!\,(n-1)!} \int_X^T e^{-(T-z)/a}\, z^{n-1}\, e^{-z/a}\, dz$$

$$= \frac{a}{b}\, e^{-bX}\,\Sigma_1 - A\Sigma_2 - C\Sigma_3 + D\Sigma_4$$

The following solutions for the second time interval are obtained by substituting the results of the convolutions in equations 25 and 26

$$F(X,T) = T/ab + 1/ab^2(e^{-bT} - 1)$$

$$- \frac{e^{-X}}{a}\left[(T + \Sigma_1)\,\frac{e^{-bX}}{b} + A(e^{-bT} + \Sigma_2) - B(1 + \Sigma_3)\right]$$

$$F(X,T) = T/ab + 1/ab^2(e^{-bT} - 1) - \frac{e^{-X}}{ab}\left[(T + \Sigma_1)e^{-bX} + (X + 1/b)(e^{-bT} + \Sigma_2) - (2X + 1/b)(1 + \Sigma_3)\right] \quad 27$$

and

$$\begin{aligned} M(X,T) &= T/ab - 1/a^2b^2(e^{-bT} - 1) \\ &\quad - \frac{e^{-X}}{a^2}\left[(T + \Sigma_1)\frac{a}{b}e^{-bX} - A(e^{-bT} + \Sigma_2) - C(1 + \Sigma_3) + D(e^{-T/a} + \Sigma_4)\right] \\ &= T/ab - 1/a^2b^2(e^{-bT} - 1) - \frac{e^{-X}}{ab}\left[(T + \Sigma_1)e^{-bX} - (X/a + 1/ab)(e^{-bT} + \Sigma_2)\right. \\ &\quad - e^{-bX}[(2X + 1/b) + a](1 + \Sigma_3) \\ &\quad \left. + [e^{-X}(X/a + 1/ab - X + a) + e^{-bX}(2X + 1/b)](e^{-T/a} + \Sigma_4)\right]. \end{aligned} \quad 28$$

All of the above integrals are of the form

$$\int z^n e^{az}\,dz = e^{az}\left[\frac{z^n}{a} - \frac{n\,z^{n-1}}{a^2} + \frac{n(n-1)\,z^{n-2}}{a^3} - \cdots + (-1)^{n-1}\frac{n!\,x}{a^n} + (-1)^n\frac{n!}{a^{n+1}}\right],$$

so that Σ_1, Σ_2, Σ_3 and Σ_4 involve combinations of series which would be difficult to evaluate without a digital computer. For that reason a numerical solution of these equations was not attempted.

It has not been possible to show that this solution converges to a steady state solution for $T \rightarrow \infty$ because of the appearance of T in the infinite series terms. However, a partial check of the final solution is provided by substituting $X = 0$ which gives back the boundary conditions $F(0,T) = 0$ and $M(0,T) = 1 - e^{-T/a}$.

The evaluation of the infinite series terms would amount to a tremendous undertaking without a high-speed digital computer. The series terms derived here can probably be manipulated to match the series terms given by Clark et al, (10,11) which were computed for a range of parameters on the M.I.T.-I.B.M. digital computer.

In gas-cooled reactors, the value of "a" may be quite large for the low-power research models but becomes smaller and approaches one for power reactors. Equations 27 and 28 indicate that the effect of decreasing "a" is to increase the initial rate of temperature response.

NUMERICAL SOLUTION

The analytical solutions of equations 11 and 12 are so complex that a numerical solution is of more value when a digital computer is not available. Solution of the equations by a finite difference method was accomplished by Bankston(14) as a special problem for the Department of Mechanical Engineering, University of New Mexico. This investigation was in progress at that time and parameters were chosen to be

compatible with the experimental equipment to be described later.

In Bankston's calculation the coolant flow selected was 10 cfm of standard air at a pressure of 75 psig. The power transient was 30.9 watts/inch. Bulk fluid properties were evaluated at 300°F and film properties for calculating the heat transfer coefficient were evaluated at 400°F. The heat transfer coefficient was evaluated from

$$\frac{hD}{k} = 0.23\left(\frac{DG}{\mu}\right)^{0.8}\left(\frac{c_p\mu}{k}\right)^{0.4} \qquad 29$$

where new symbols are

D = inside tube diameter

k = thermal conductivity

G = mass velocity = w/A_f

μ = viscosity

From the above specifications, the following values for the similarity numbers were computed:

M = 3.88×10^{-3} m where m is the metal temperature in °F;

F = 3.88×10^{-3} f where f is the fluid temperature in °F;

X = 0.437 x where x is distance on the tube in feet;

T = 19.7 t where t is time in seconds; and

$$a = 265 = \frac{\gamma_m c_m A_m}{\gamma_f c_f A_f}$$

The relatively large value of "a" causes the temperature change during the first time interval to be only 2.88°F at x = 6 feet where the steady state temperature ($t \to \infty$) is 932°F. It is apparent that solution may begin with the

equations for the second time interval and assumed initial metal and fluid temperatures of zero.

The convergence criteria for determining the size of Δx and Δt was not found but on the basis of judgement, convenience and an estimate of the error, the choice was $\Delta x = 1/2$ foot and $\Delta t = 5$ seconds.

The calculations used a finite difference rectangular grid in the X,T plane with nodes at intervals of ΔX and ΔT. The nodal temperatures represented the average temperature of a section of length ΔX during the time interval ΔT. The finite difference equations were derived from the non-dimensional differential equations 11 and 12, and involved both M and F at four adjacent nodes. The solution starts with the initial and boundary conditions which provide M and F at three of the nodes. The two finite difference equations provide M and F at the fourth node. The procedure was continued to X = 2.622 and T = 2500.

The method employed is straightforward and relatively simple but the actual work is long and tedious. Since each calculation depends on all previous calculations, computation errors are a serious threat. The major disadvantage of this type of numerical calculation is that the entire process may have to be repeated in order to demonstrate the effect of a new ratio of heat capacities, "a." Without convergence criteria the accuracy of the results is slightly uncertain.

The results of this numerical calculation are compared with experimentally determined temperatures in a later section.

CHAPTER 4

EXPERIMENTAL INVESTIGATION

The theoretical investigation in the preceding chapter resulted in analytical and numerical solutions for the metal and bulk temperatures as functions of length and time. The necessary assumptions and complexity of the analytical solution and the time-consuming quality of the numerical solution suggest experimental methods. A thermal analog of the reactor coolant channel has the advantage that actual thermodynamic changes in properties are included. This may lead to fewer restrictions than required by the theoretical methods and give greater confidence in the results. A disadvantage is that construction of the model, data reduction, and analysis of results are also quite time consuming.

APPARATUS

The analog investigated here was a thin-walled metal tube which was heated by its resistance to the flow of electrical current. The coolant was air at 75 psig. Temperatures were detected by thermocouples placed at various places along the tube and at the coolant exit. Thermocouple outputs were recorded on an oscillograph. The power supply was a d.c. arc welder and an approximate step function change in heat generation was produced by completing the circuit with a knife switch.

An overall picture of the heated tube and associated equipment is shown in Figure 2. Details of the lower end of the heated tube are shown in Figure 3. This picture shows two

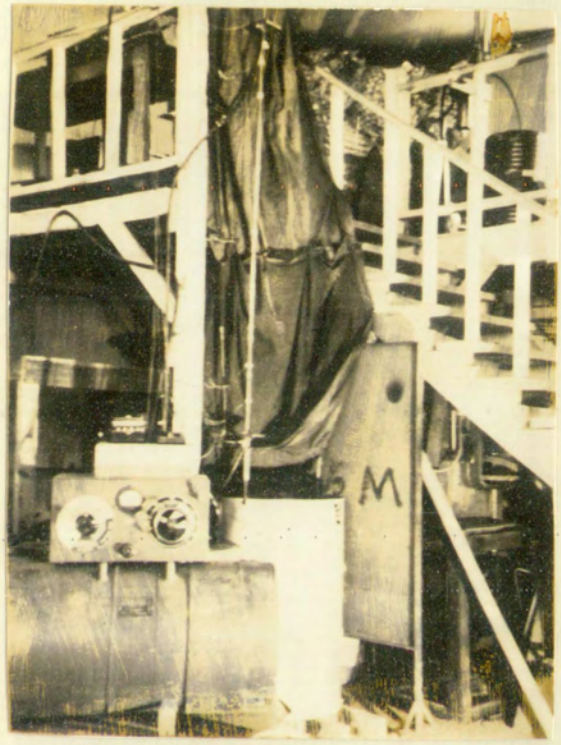

Figure 2 Overall View of Heated Tube

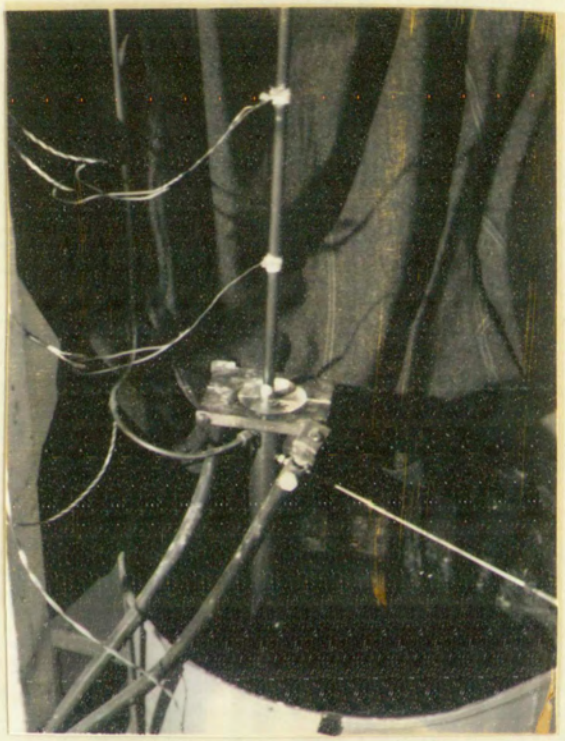

Figure 3 Detail of Electrode and Thermocouples

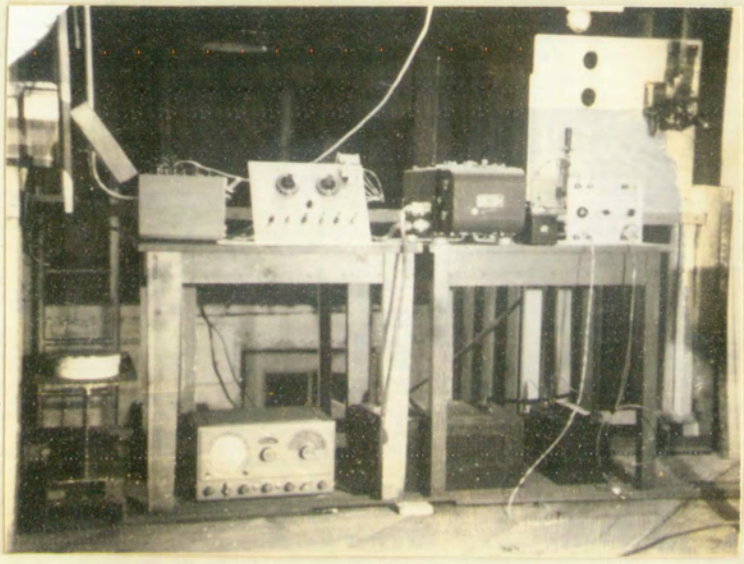

Figure 4 Associated Instrumentation

thermocouples installed on the tube, one of the electrical contacts, and the coolant temperature probe. Additional instrumentation is shown in an overall view in Figure 4.

The experimental data obtained were for three levels of heat generation and for three coolant flow rates. Other variables were maintained in agreement with the specification for the numerical solution. Four runs were made for the heat generation level and flow rate corresponding to the numerical solution specification. Two runs each were made of the other four experimental conditions.

Heat Exchanger -- The test section was an Inconel metal tube 6 feet long, 1/2 inch o.d. and 0.035 inch wall thickness. This simulated the reactor fuel element. Inconel was chosen because it has a relatively high electrical resistivity (100 μ - ohm-cm) which does not change appreciably with changes in temperature. It also has high strength properties at high temperatures.

A three foot length of tube at the inlet end was left unheated for the development of a stable turbulent flow pattern. This corresponds to $L/D \cong 85$ which is more than sufficient to minimize starting effects on the heat transfer coefficient.

Air System -- The coolant for the analog was air supplied by the compressed air system in the Mechanical Engineering shop. Two pressure regulators reduced and regulated the inlet air pressure to the heated tube. One of the regulators also incorporated an oil and water separator which removed most of the

moisture from the coolant, however, there was evidence of a slight amount of moisture in the test section.

The flow rate was determined by measuring the pressure drop across a sharp-edged orifice. The design of the orifice and its discharge coefficients were taken from the publication by Grace and Lapple(19). A 36-inch water manometer with a least division of 0.1 inch was used to obtain accurate differential pressure readings. Variations in flow rate during a run were observed to be on the order of 3%.

Inlet pressure to the test section was measured with a conventional pressure gauge. Pressure variations were on the order of 5%. Inlet air temperature was monitored by a mercury thermometer inserted in a well in the inlet piping.

The downstream end of the test section terminated in a 12 inch length of 1 inch stainless steel pipe. Access to this chamber was provided by two tapped holes; one located 3/4 inch and the other about 8-3/4 inch downstream from the end of the heated tube. The original intent of this chamber was to obtain a better measurement of the coolant bulk temperature by insuring mixing in an unheated region. Lack of time prevented utilizing the chamber except for the mounting of the coolant temperature probe in the upstream access hole.

Air leaving the mixing chamber passed through about 50 feet of coiled 1/2 inch copper tubing which was immersed in a barrel of water. Thus, hot air leaving the analog was cooled to room temperature before reaching the flow-rate controlling valve at

the end of the system.

Electrical Power System -- The electrical power circuit diagram is shown in Figure 14 in the Appendix.

Power for heating the analog was provided by a DC welder power supply. Since this was an AC-DC motor-generator set, isolation from ground was provided. Current measurement was accomplished with a new 50 mv.-200 ampere shunt and a 0-100 millivoltmeter with a least division of one millivolt. Voltage was measured with a 0-30 voltmeter with a least division of 0.5 volts. Both meters were calibrated against a standard cell prior to the experiments.

Circuit closing was done with a knife-switch. The circuit was opened with a circuit breaker which also provided protection against accidental shorts. Difficulty was experienced in obtaining a consistent power level from the generator. This was overcome by providing an attendant to continually adjust the welder controls during the experimental runs. Some power fluctuation resulted but the effect is significant only during the first few seconds of each run.

An effort was made to nullify the effect of the heat capacity associated with the electrical contacts on the tube. The contactor developed was intended to be self-heating so that there would be a negligible temperature gradient between the tube and the contact and hence no heat loss.

A view of this contactor is shown in Figure 3. A 3 inch disc of Incoloy with a concentric hole of 1/4 inch radius was machined to a thickness of 1/32 inch for all radii greater than 1/2 inch. The thickness at the edge of the hole which contacted the tube was 1/8 inch. Between the edge of the hole and the 1/2 inch radius, the thickness decreased uniformly to 1/32 inch. The disc was then split across a diameter and the two halves soldered to copper blocks. In use, the two halves of the disc were assembled around the Inconel tube and clamped in place by studs through the copper blocks. Electrical leads were attached to the copper so that current would flow through the disc to the tube and the disc would be heated by the I^2R loss within it.

The effectiveness of this contact was not fully investigated.

Thermocouples -- Chromel-alumel thermocouples were chosen for measuring tube temperatures at the lower end of the tube because of their suitability for high temperature applications. Because of the superior thermal e.m.f., iron-constantan thermocouples were used for the three measurements on the upper portion of the tube where lower temperatures were expected. All thermocouples were made from 26 gage wire.

The attachment of the thermocouples to the tube was the subject of some investigation. Attempts to provide a metallic bond failed because of difficulties in welding the dissimilar materials and because of stray electrical effects. The following technique was finally used: First, a thin layer of seriesen

ceramic cement was applied in a half-inch-wide strip three-quarters of the way around the tube. Each wire of the thermocouple pair was placed on the tube so that it was electrically insulated by the ceramic layer. The properly cleaned ends were twisted tightly and welded together. The joint was clipped so as to leave about 1/8 inch of the welded junction. This junction was then bent up to lay against the tube. A strip of 1/2 inch glass tape was tightly wrapped twice around the tube over the thermocouple joint and tied at the back. A piece of 26 gauge wire was wrapped once around the tube over the junction and fastened by twisting the ends together at the back. The wire held the thermocouple tightly against the tube.

Impedance matching considerations required that the thermocouple circuit have a minimum electrical resistance. Since the thermocouple materials have relatively high resistance, only a minimum length was used. Rough calculations indicated that the end of a six-inch length would not be affected by heat conduction from the hot junction. Copper leads were used beyond the end of the six inch length and the lead-to-thermocouple splice became the reference junction. The reference junction temperature was assumed to be at room temperature.

The adequacy of the thermocouple installation was demonstrated by steady state tests using a thermometer well clamped on to the tube over the thermocouple. Temperature readings were compared at equilibrium and during the cooling period

following removal of power. Excellent agreement of the temperatures indicated by the thermocouple and the thermometer was observed. This data is shown in Table 1 in the Appendix.

Fluid temperature was detected by means of an iron-constantan thermocouple probe constructed by Pratt and Whitney Aircraft Co. The probe consists of a 1/8 inch diameter stainless steel tube which encases the thermocouple wire. The probe was installed in the upper access hole of the mixing chamber. It was inserted so that the thermocouple junction was centered in the stream of air leaving the heated tube.

Oscillograph -- The output e.m.f. of the various thermocouples was detected by the galvanometers in a Hathway Type S-12A Oscillograph. The galvanometer traces were recorded on photographic paper moving at a speed of 1/2 inch/sec. A time marker system within the oscillograph provided marks on the paper at intervals of 1/10 second so that the time dependence of all temperatures could be accurately determined. The time marker was compared to a 60 cycle/sec signal and found to be extremely accurate.

CALIBRATION

Independent calibration of the individual galvanometers was not possible since they have a relatively small internal impedance (about 7 ohms). When connected to a thermocouple the power developed within them is greatly influenced by the impedance of the external circuit. This made it necessary to

calibrate the oscillograph galvanometer while they were connected with their thermocouples. To accomplish this, a switching circuit was devised so that a known e.m.f could be applied in series with the galvanometer-thermocouple circuit. A portion of the switching circuit is shown schematically in Figure 15 in the Appendix. This part is typical of the six independent circuits required for the six thermocouples.

The source of known e.m.f. was obtained by constructing a voltage divider circuit. The schematic diagram of this calibrating circuit is shown in Figure 16 in the Appendix. A 12 volt storage battery was used as the prime source of electrical power. Ten voltage steps were provided by using five taps in a series resistance circuit and a high-low range switch.

The actual output voltage of this circuit would depend upon the output impedance. Since each galvanometer-thermocouple circuit has a different impedance, it was necessary to put the circuit to be calibrated into a leg of a Wheatstone bridge. The bridge is balanced by adjusting resistors which shunt the galvanometer circuit. The voltage divider then feeds the bridge which, when balanced, always constitutes the same impedance. Since the other three legs of the bridge are fixed, the voltage across the galvanometer is also fixed.

The voltage corresponding to each step was determined by comparison on a Leeds and Northrup No. 8662 Portable Precision Potentiometer.

The resistance of the fluid temperature probe was about the same magnitude as the resistance of the galvanometer. It was evident that only half of the power resulting from the thermal e.m.f. would be developed in the galvanometer. This was overcome by the use of a low-level current amplifier designed by Summers(20) which matched impedances and provided some amplification. A schematic of this amplifier is presented in Figure 17 in the Appendix.

After carefully determining the output voltages for each step of the calibrating circuit, the galvanometer-thermocouple circuits were calibrated in turn with the corresponding galvanometer deflection being recorded on the oscillograph record. A typical calibration plot of deflection versus applied e.m.f. is shown in Figure 18 in the Appendix. It will be noted that the response is essentially linear over the range of interest. The assumption that the e.m.f. output of the thermocouples used is directly proportional to temperature is within the accuracy required here. Then the conversion from galvanometer trace deflection to temperature is simply temperature = K(deflection) where K must be determined for each circuit. The K's determined are tabulated in Table 2 in the Appendix.

EXTERNAL HEAT LOSSES

The external surface of the heated tube was not insulated and heat transferred from this surface was found to be appreciable. This loss was found experimentally by measuring the equilibrium temperature at each thermocouple location when a

measured amount of power was delivered to the tube and there was no coolant flow. Under these conditions, essentially all of the input power is dissipated at the outer tube surface. Conduction loss at the ends is quite small since the cross-section is small. Data from this experiment is presented in Table 3 in the Appendix. A plot of surface temperature versus heat loss is shown in Figure 19 in the Appendix. Curves are presented for several distances down the tube from the inlet end. Heat loss is somewhat greater at the upper end of the tube because of the greater natural convection velocity.

During this experiment, the thermal e.m.f. was measured on the precision potentiometer and was also recorded on the oscillograph. This provided an additional check on galvanometer calibration and is indicated in Figure 18 in the Appendix.

EXPERIMENTAL TESTS

An outline of the procedure followed in performing an experimental run follows: The coolant flow conditions were carefully set up. The oscillograph was started and the knife-switch closed to start heat generation in the tube. Galvanometer traces were observed on the viewing screen of the oscillograph and were photographically recorded. When no further deflection could be detected, the oscillograph was shut off. The portable precision potentiometer was connected to the calibrating input terminals of the thermocouples switching circuit (Figure 15) and the thermal e.m.f. was measured

directly for each thermocouple. Input power was recorded.

A total of six experimental tests were made. Two runs were made for each test.

The inlet air pressure was 75 psig in all of the tests. This results in a similarity number "a" of 265 and corresponds to the "a" used in computing the numerical solution. The tests involved significant variations in the input power and air flow rate only. The following is a summary of the experimental conditions for each test:

Test No. 1, w = 0.865 lb/min, input power = 30.9 watts/in.
Test No. 2, w = 0.708 lb/min, input power = 30.9 watts/in.
Test No. 3, w = 0.500 lb/min, input power = 30.9 watts/in.
Test No. 4, w = 0.865 lb/min, input power = 13.9 watts/in.
Test No. 5, w = 0.865 lb/min, input power = 41.6 watts/in.
Test No. 6, w = 0.865 lb/min, input power = 30.9 watts/in.

DATA REDUCTION

After developing the oscillograph record, selected times after the beginning of the power transient were located. A set of proportional dividers were set up to give the proper conversion from deflection to temperature as indicated by Table 2. The temperature from each thermocouple circuit was determined for the selected times and recorded. The compilation of these temperatures is presented in Tables 4 and 5 in the Appendix.

The averaged data from Table 4 was plotted on graph paper as temperature versus distance on the tube. Smooth curves were drawn through points for the same time after the beginning

of the transient. The purpose of "smoothing" the data was to minimize scattering and eliminate erratic readings. A typical example of this procedure is shown in Figure 20 in the Appendix where the smoothed curves for Test 2 are presented.

The conversion to dimensionless temperature, time and distance was required next. The values for thermal properties used in the numerical solution were assumed to be adequate. The heat transfer coefficient was previously evaluated from

$$\frac{hD}{k} = 0.23\left(\frac{DG}{\mu}\right)^{0.8}\left(\frac{c_p\mu}{k}\right)^{0.4} \qquad 29$$

where $G = w/A_f$. A flow rate correction for h can be made on the basis of equation 29 which yields the relation

$$\frac{h_1}{h_2} = \left(\frac{w_1}{w_2}\right)^{0.8} \qquad 30$$

The proper ΔU_g to use in computing the dimensionless temperatures is determined by

$$\Delta U_g = (\text{input power}) - (\text{external power loss}) \qquad 31$$

where the external power loss was determined from the "36 inch" curve of Figure 19 using the "smoothed" temperature at the location of interest. This technique is somewhat arbitrary but it may be argued that considerably more data and analytical evidence would be required to justify a different procedure.

The non-dimensional data may now be calculated using the above modifications. The resulting similarity numbers, along

with the "smoothed" temperature and external heat loss data are tabulated in Table 6 in the Appendix.

The measured fluid temperatures may be converted to non-dimensional form by a similar technique. In this case, fluid temperature was measured only at x = 72 inches. The external heat loss for correcting ΔU_g was obtained by using a temperature obtained by extrapolating the smoothed metal temperature to x = 72 inches and using the curve for "36 inches" in Figure 19 .

ERRORS

Estimates of the response time of the thermocouples was facilitated by information found in a text by Giedt(21). By extrapolation of data presented in his Table 14.1, the response of the coolant thermocouple was estimated to be t = 0.3 seconds where t is the time required for a thermocouple to reach 63.2% of a step change in temperature. The response of the tube thermocouples can be computed from

$$t = Wc/hA \qquad 32$$

where t = time to reach 63.2% of a step change, hr.

W = weight of the thermocouple, lbs.

$= \rho L \pi d^2/4$

c = specific heat, BTU/lb^{o}F

h = coefficient of heat transfer, BTU/h f^2 ^{o}F

A = surface area of thermocouple, f^2

$= \pi dL$.

This reduces to $t = \gamma dc/4h$. The following values were assumed:

$\gamma = 540$ lb/f^3

$d = 0.016$ in.

$c = 0.11$ BTU/lb ^oF

$h = 250$ BTU/h f^2 ^oF

Substitution of these values results in $t = 7.9 \times 10^{-5}$ hr = 0.28 seconds.

Trace deflections were measured to an accuracy of about $\pm$ 1/64 inches. The data reduction error = 1/64K, ranges from $\pm$ 4 to $\pm$ 18 ^oF.

CHAPTER 5

RESULTS

A summary of the results of Bankston's numerical solution is presented in Figure 5 by a graph of the similarity number M versus X for several values of T. This graph provides the necessary information for making a comparison between theory and analog results.

Tests 4, 5, and 6 investigated the effect of varying the magnitude of ΔU_g. The results of this series of tests is compiled in non-dimensional form in Table 6. The correlation of this data is shown in Figures 6, 7, and 8 where non-dimensional metal temperature, M, is plotted versus non-dimensional time, T. The three figures are for three particular values of non-dimensional distance, X.

According to the dimensional analysis, the effect of varying the flow rate should be accounted for by the similarity number X. This was investigated by Tests 1, 2, and 3. The non-dimensional data is also compiled in Table 6. Figures 9, 10 and 11 are plots of M versus T for tests 1, 2, and 3 respectively. Each graph contains the curves for three values of X. Superimposed on the experimental curves are the theoretical curves for the same values of X. These theoretical curves are drawn from information presented by Figure 6 as mentioned above.

The averaged fluid temperatures from Tests 1 and 6 were converted to non-dimensional temperature, F, and compiled in Table 7 in the Appendix. Figure 12 is a plot of F versus T

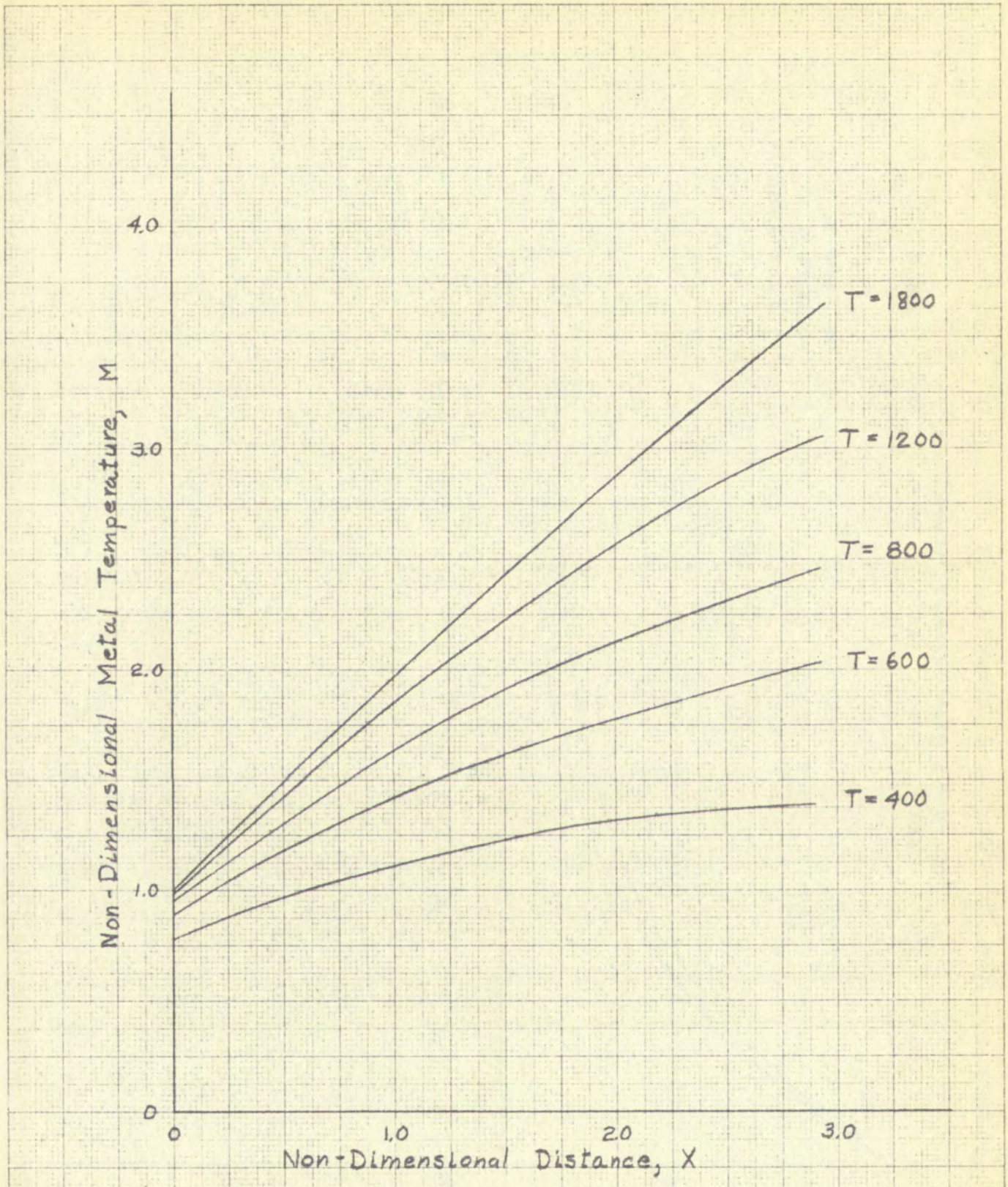

FIGURE 5 SUMMARY OF METAL TEMPERATURE FROM NUMERICAL SOLUTION

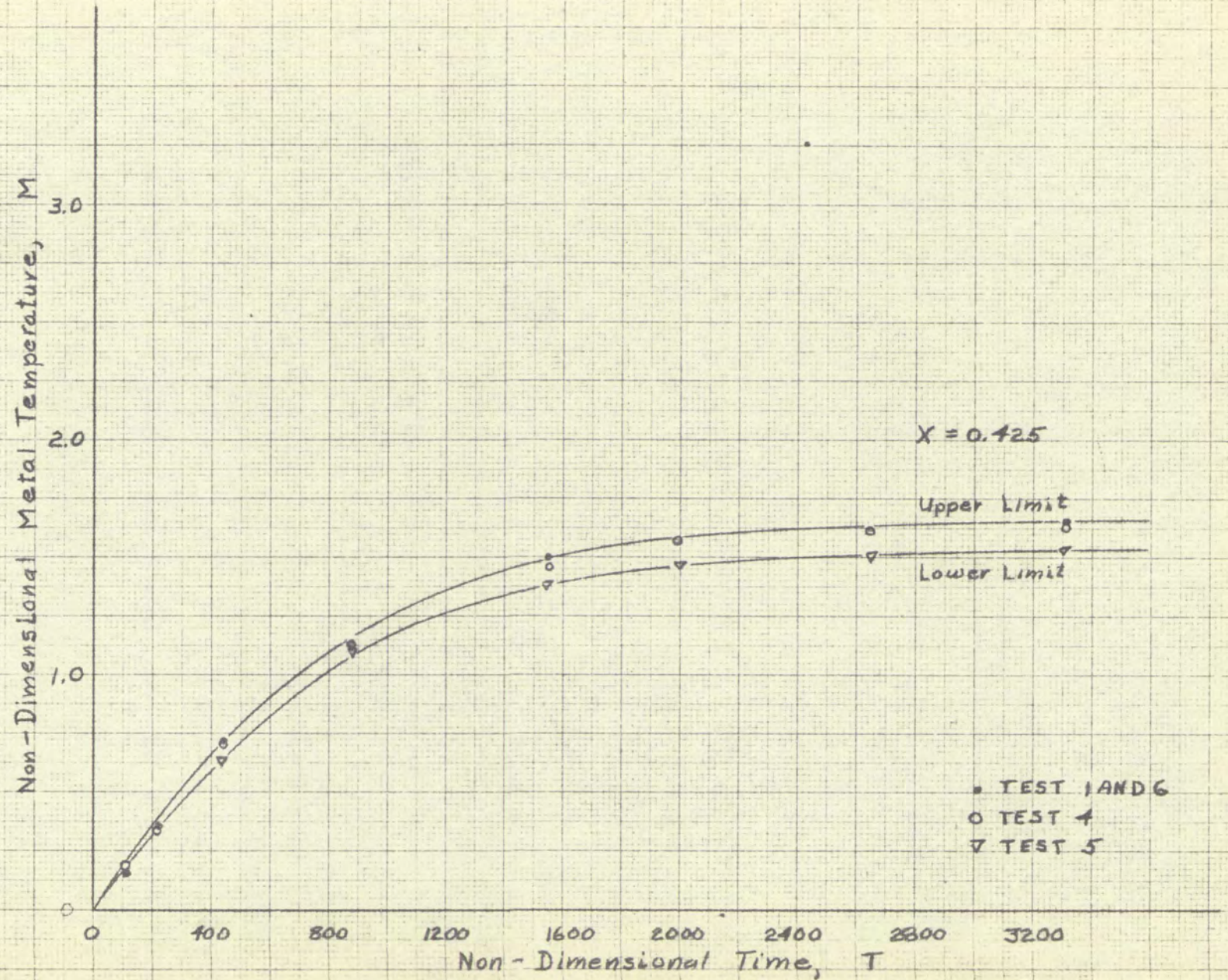

FIGURE 6 NON-DIMENSIONAL TEMPERATURE VS. TIME FOR TESTS 4, 5, 6

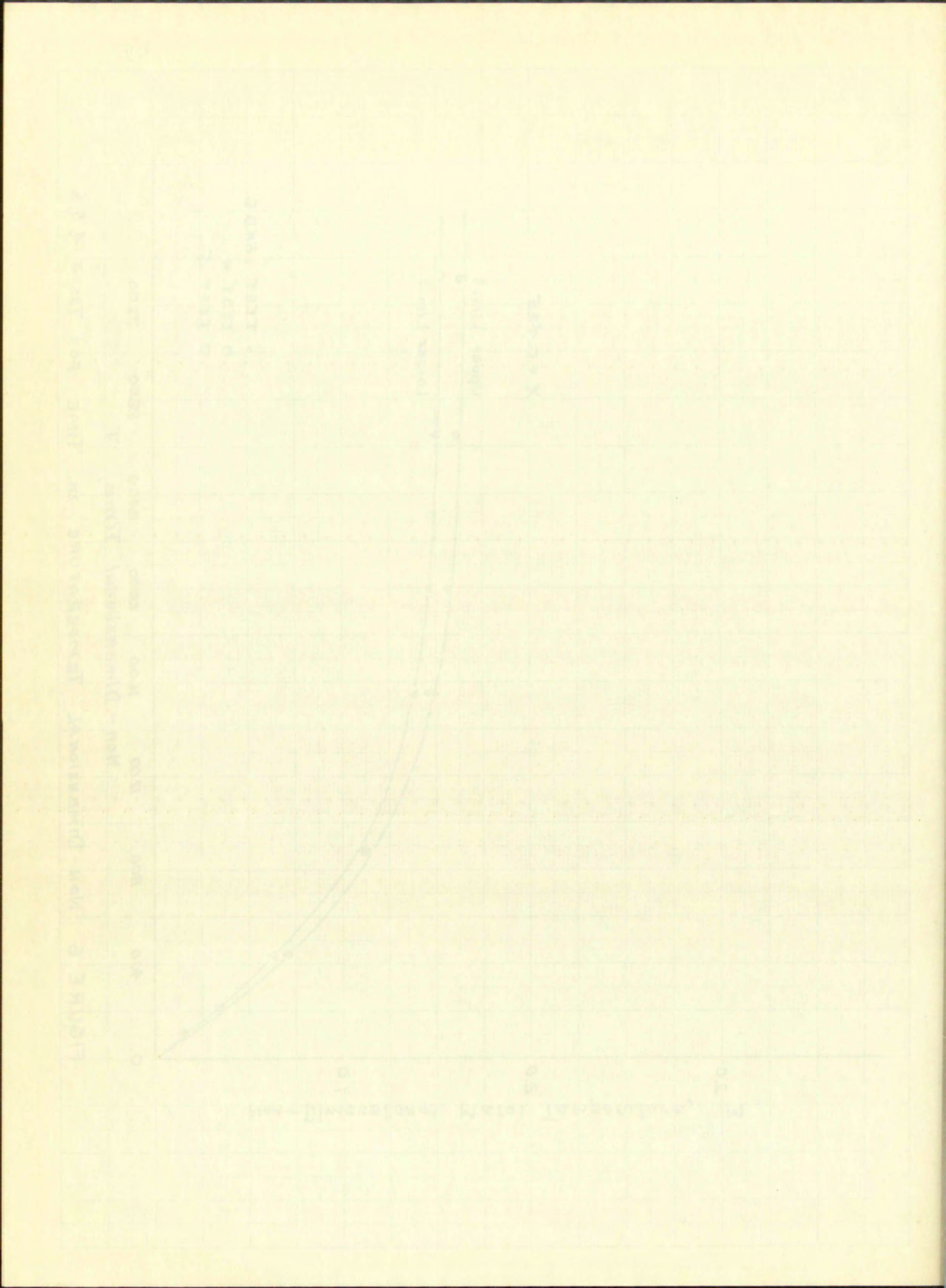

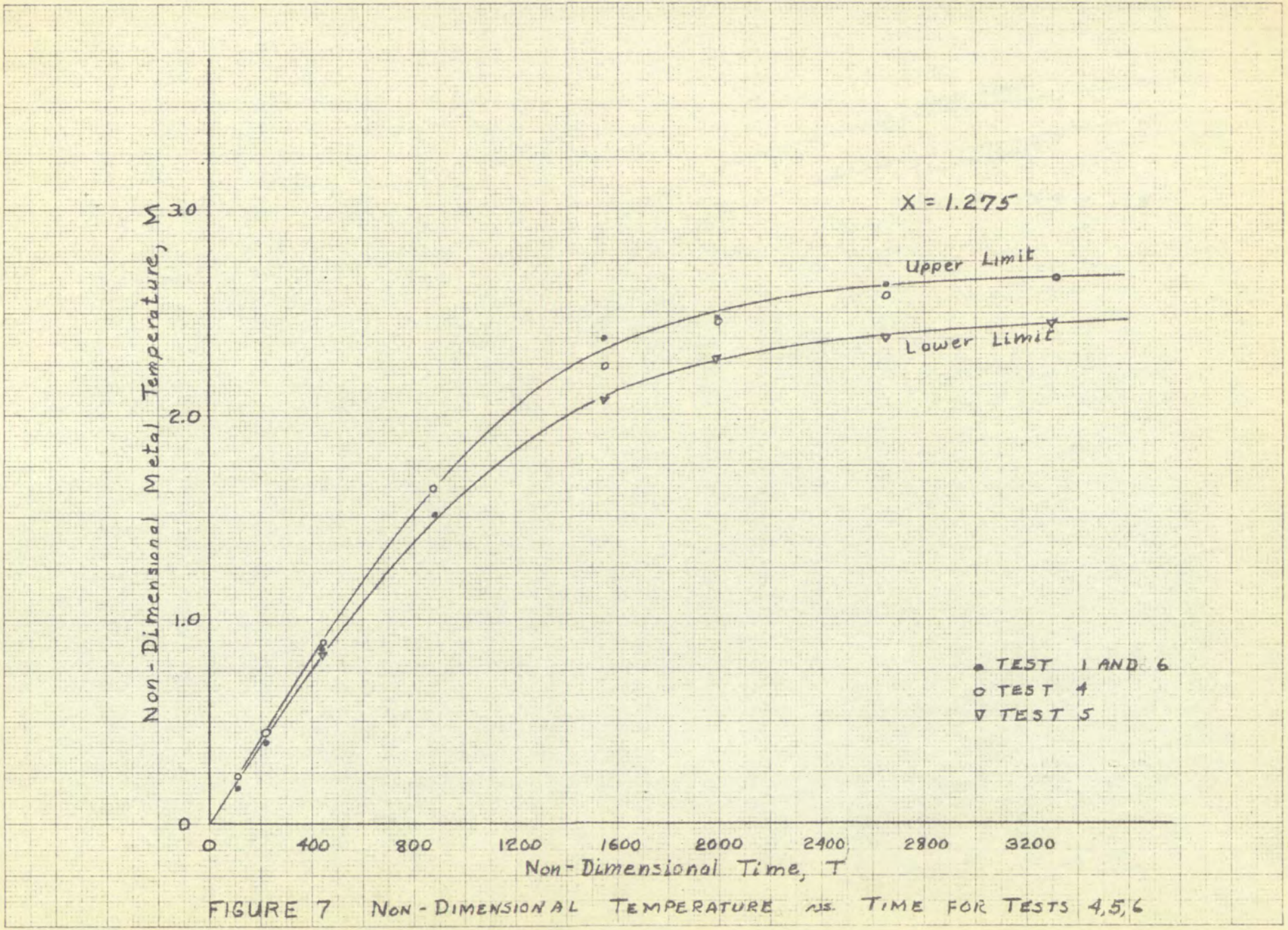

FIGURE 7 NON-DIMENSIONAL TEMPERATURE vs. TIME FOR TESTS 4,5,6

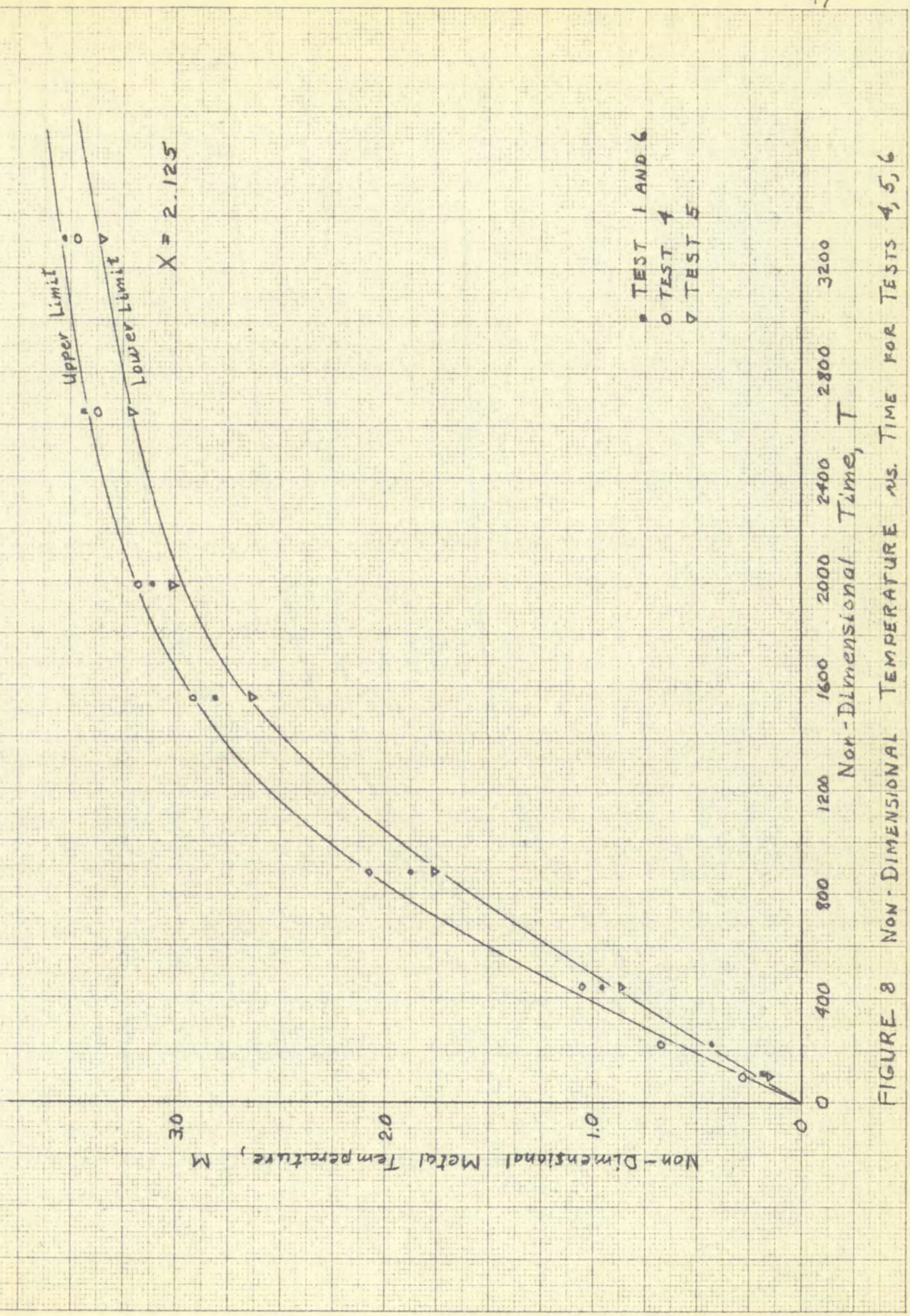

FIGURE 8 NON-DIMENSIONAL TEMPERATURE VS. TIME FOR TESTS 4, 5, 6

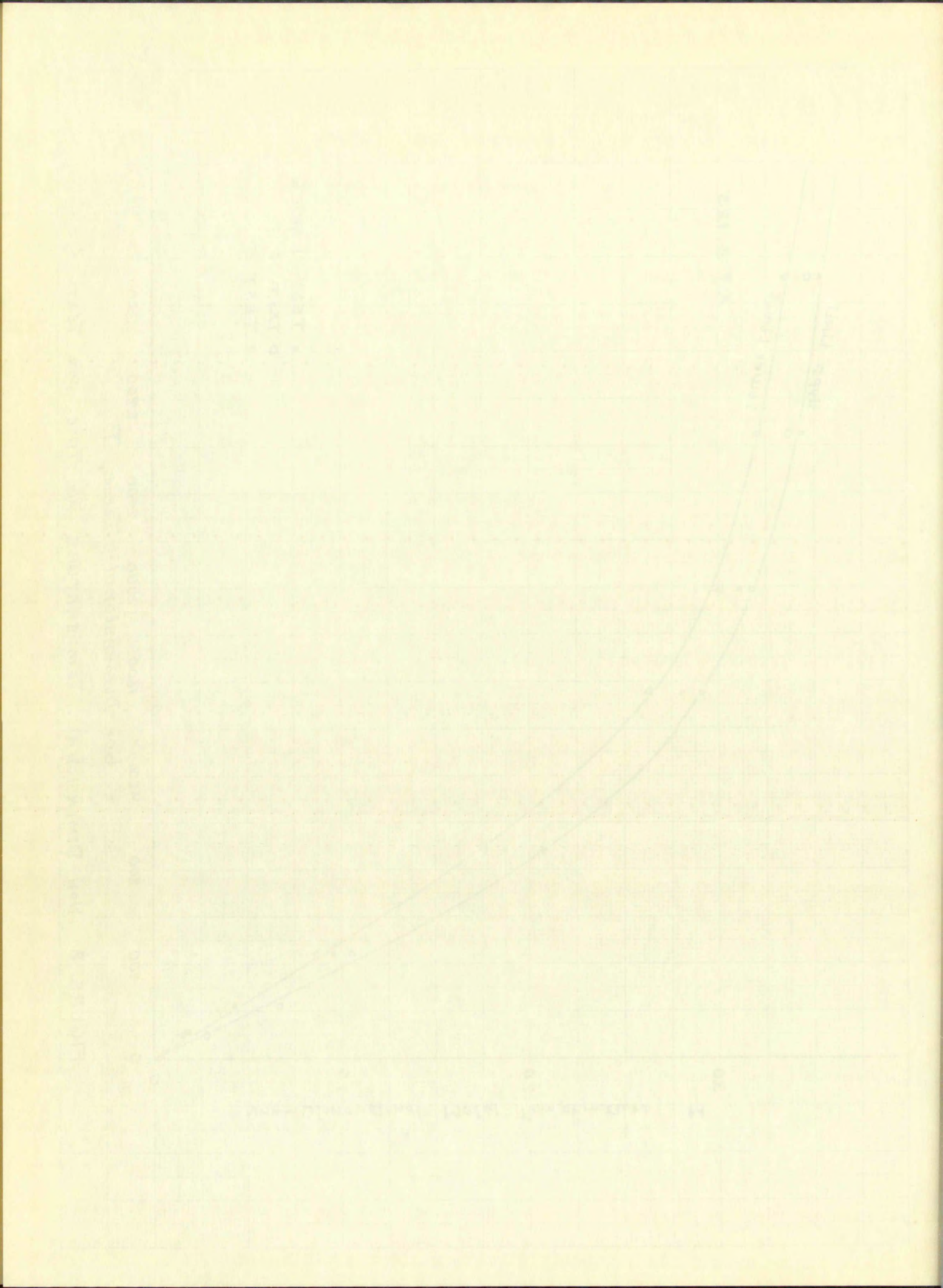

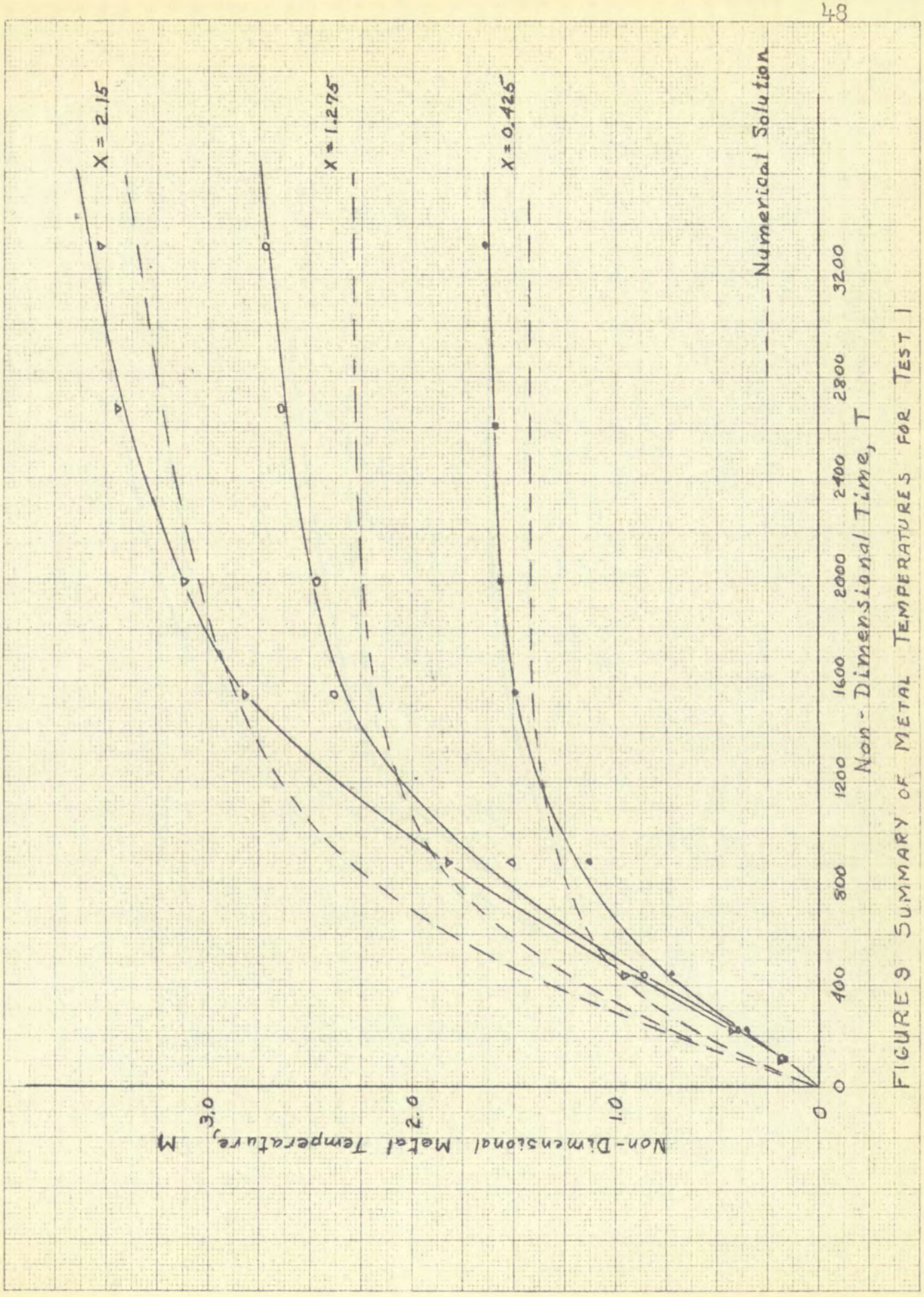

FIGURE 9 SUMMARY OF METAL TEMPERATURES FOR TEST 1

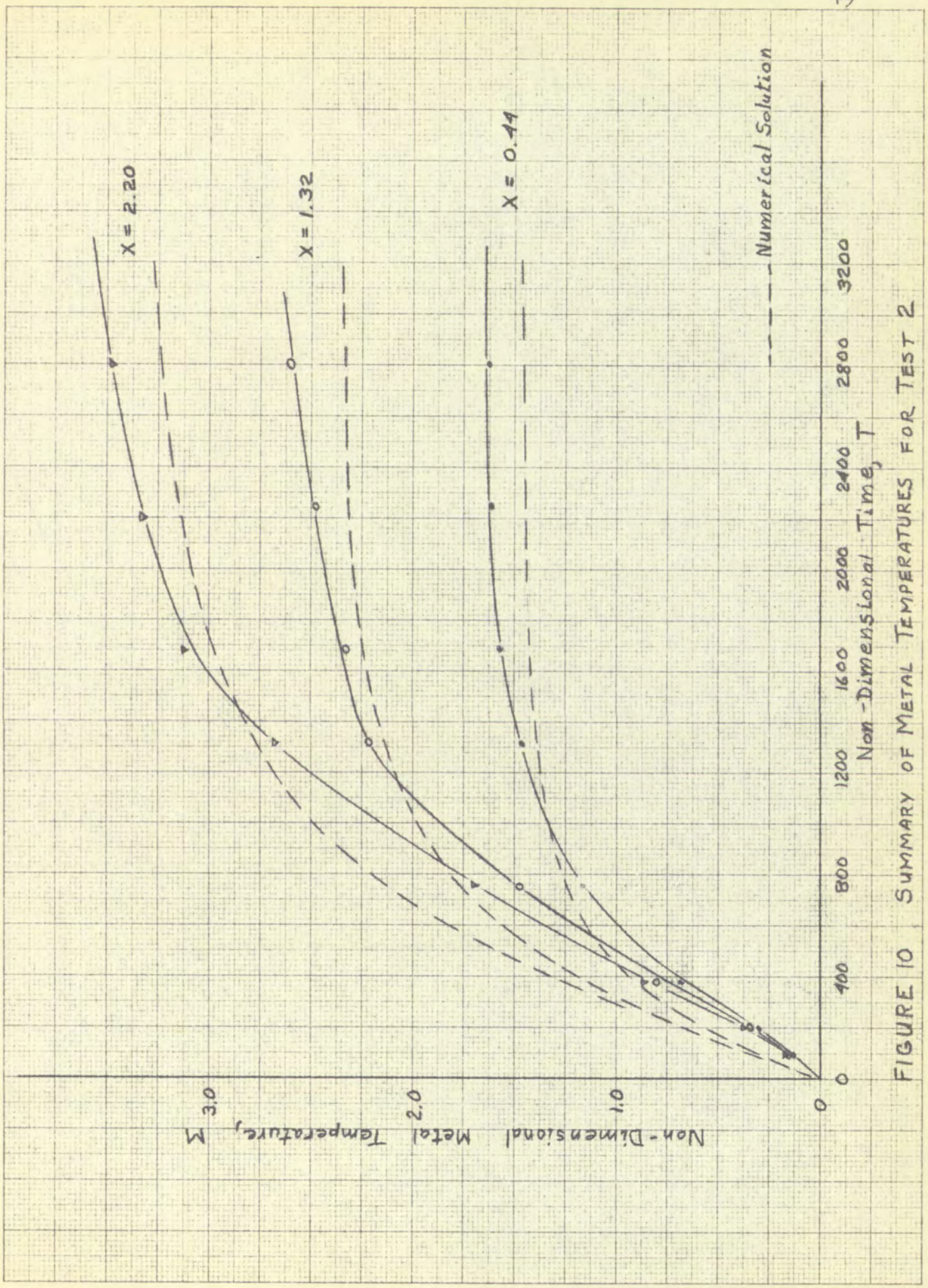

FIGURE 10 SUMMARY OF METAL TEMPERATURES FOR TEST 2

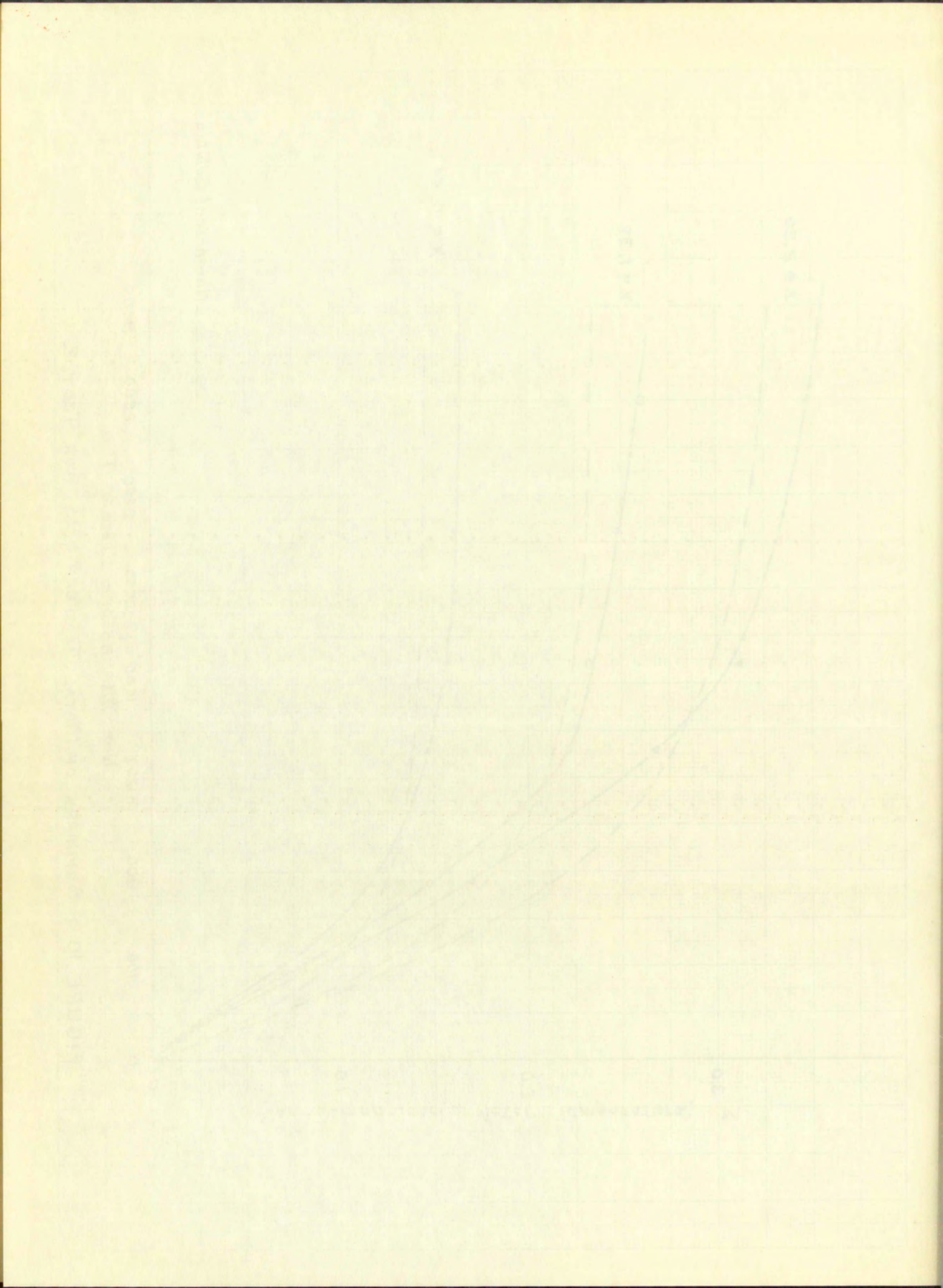

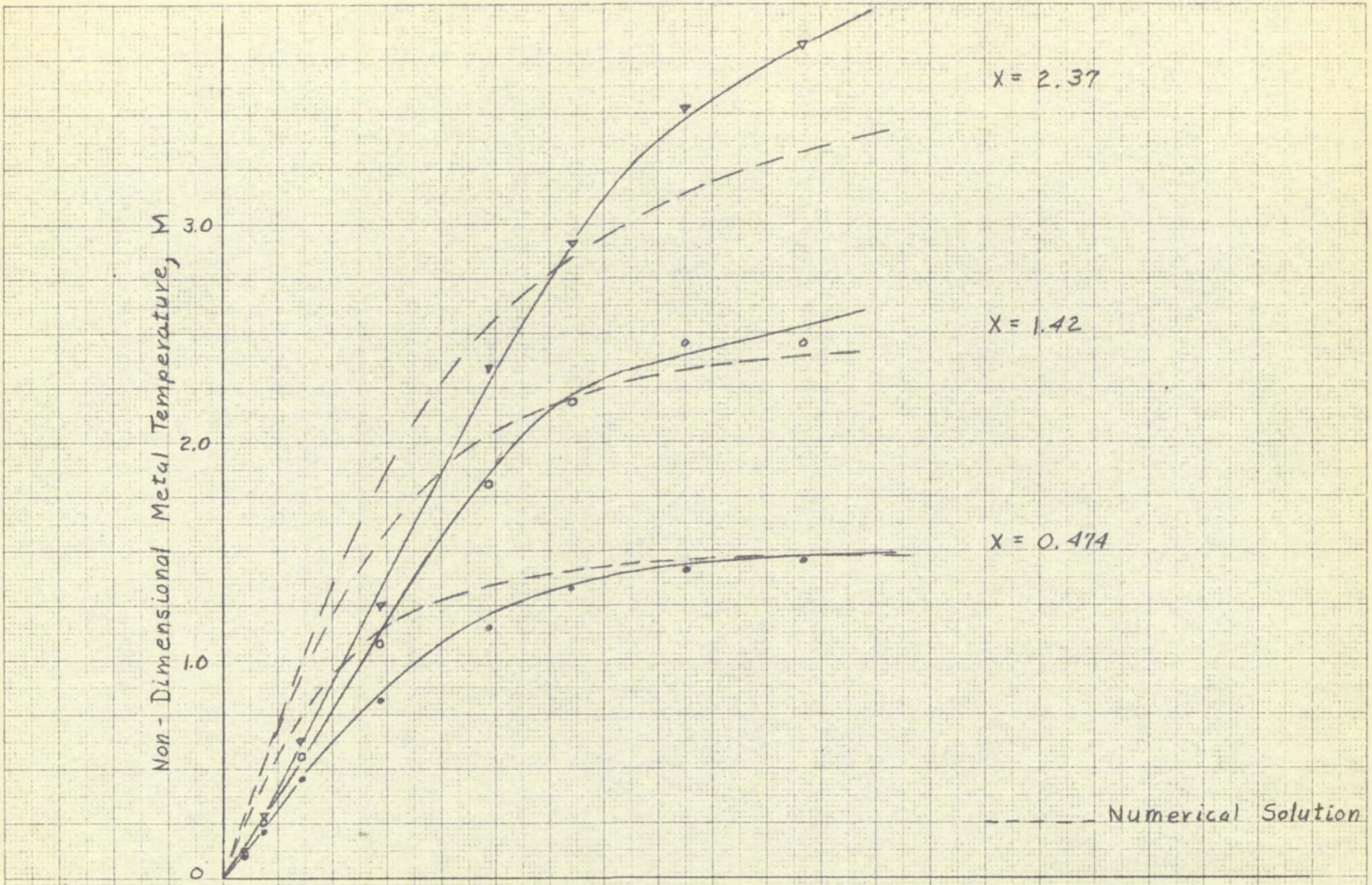

FIGURE 11 SUMMARY OF METAL TEMPERATURES FOR TEST 3

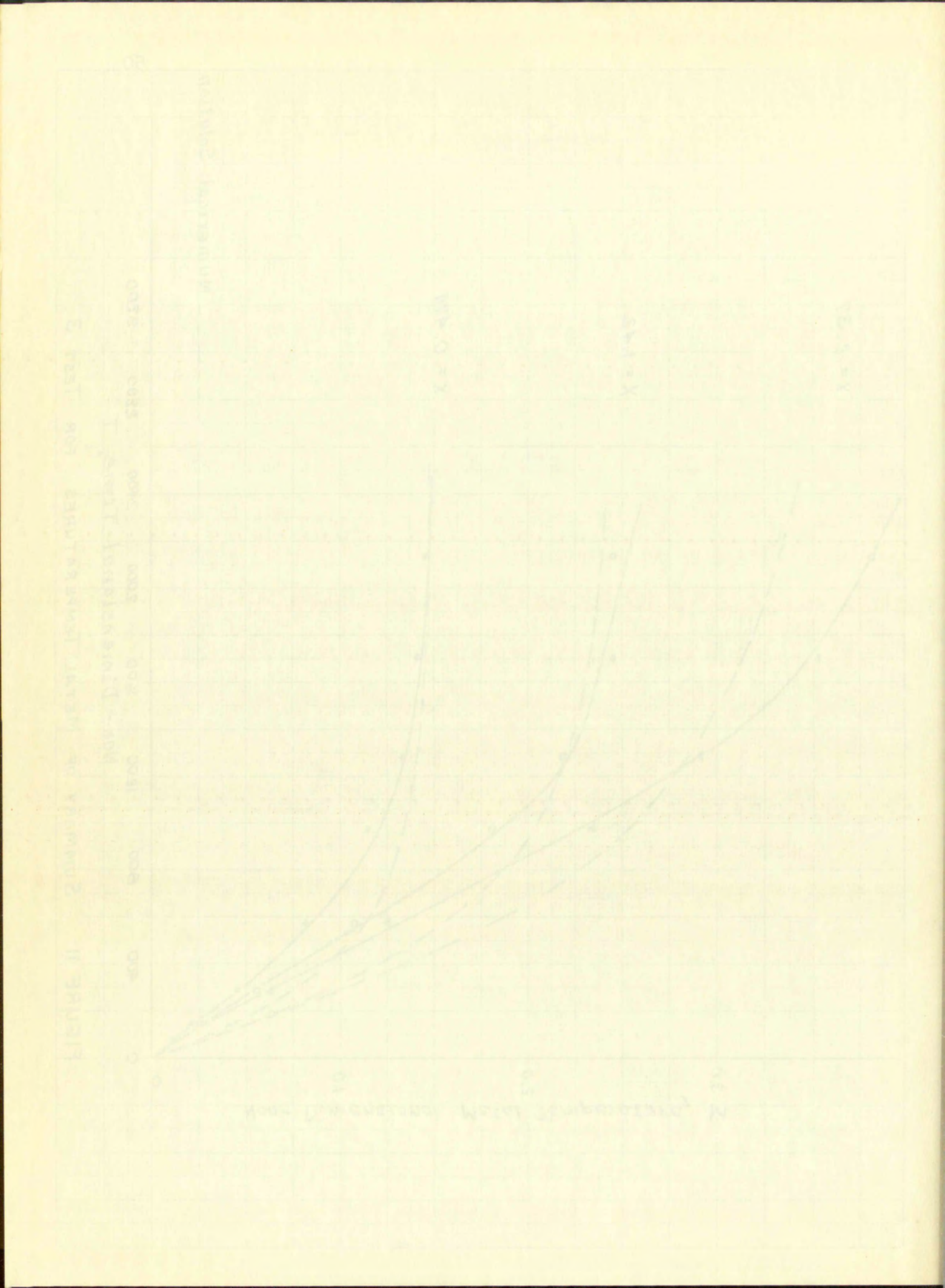

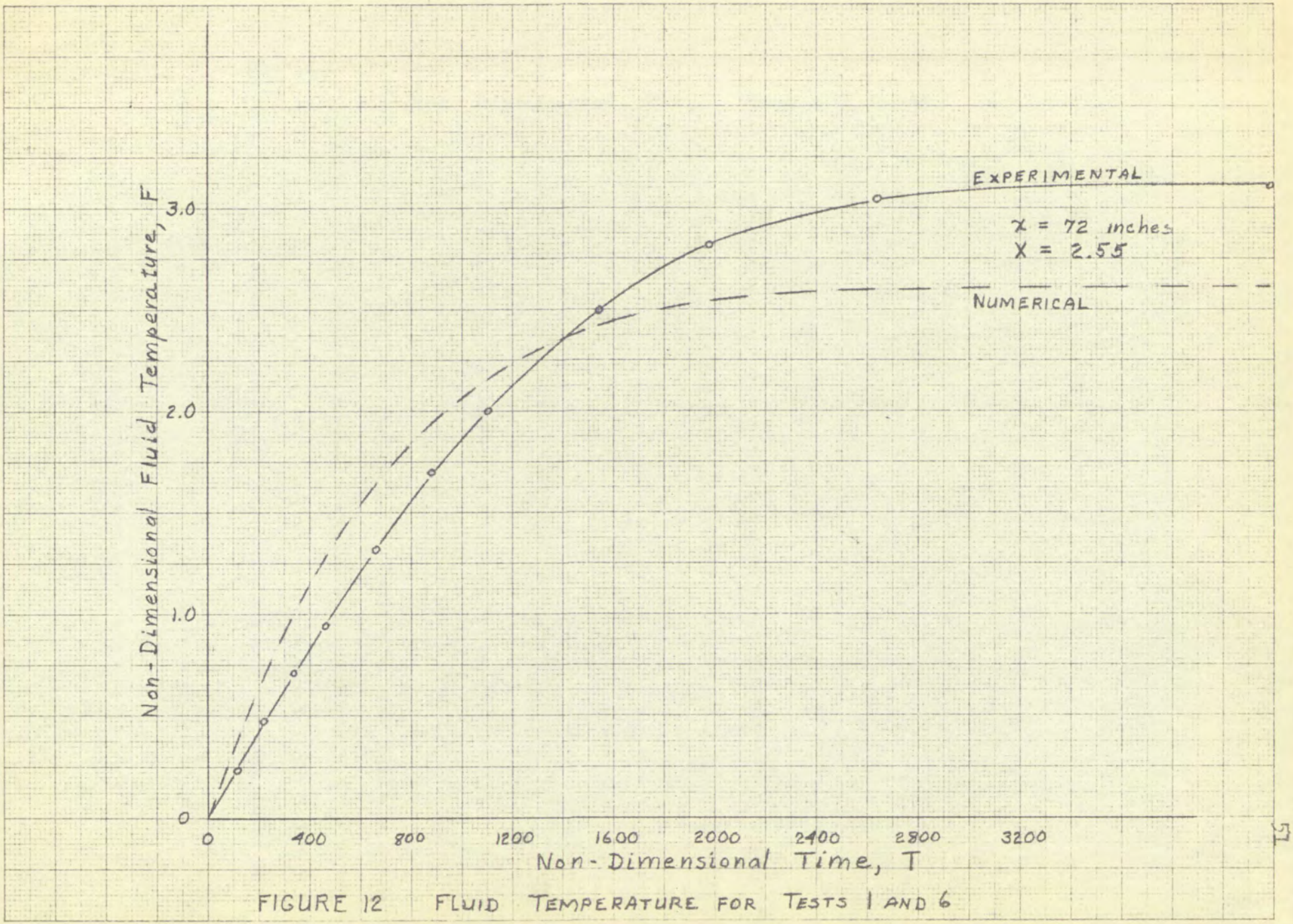

FIGURE 12 FLUID TEMPERATURE FOR TESTS 1 AND 6

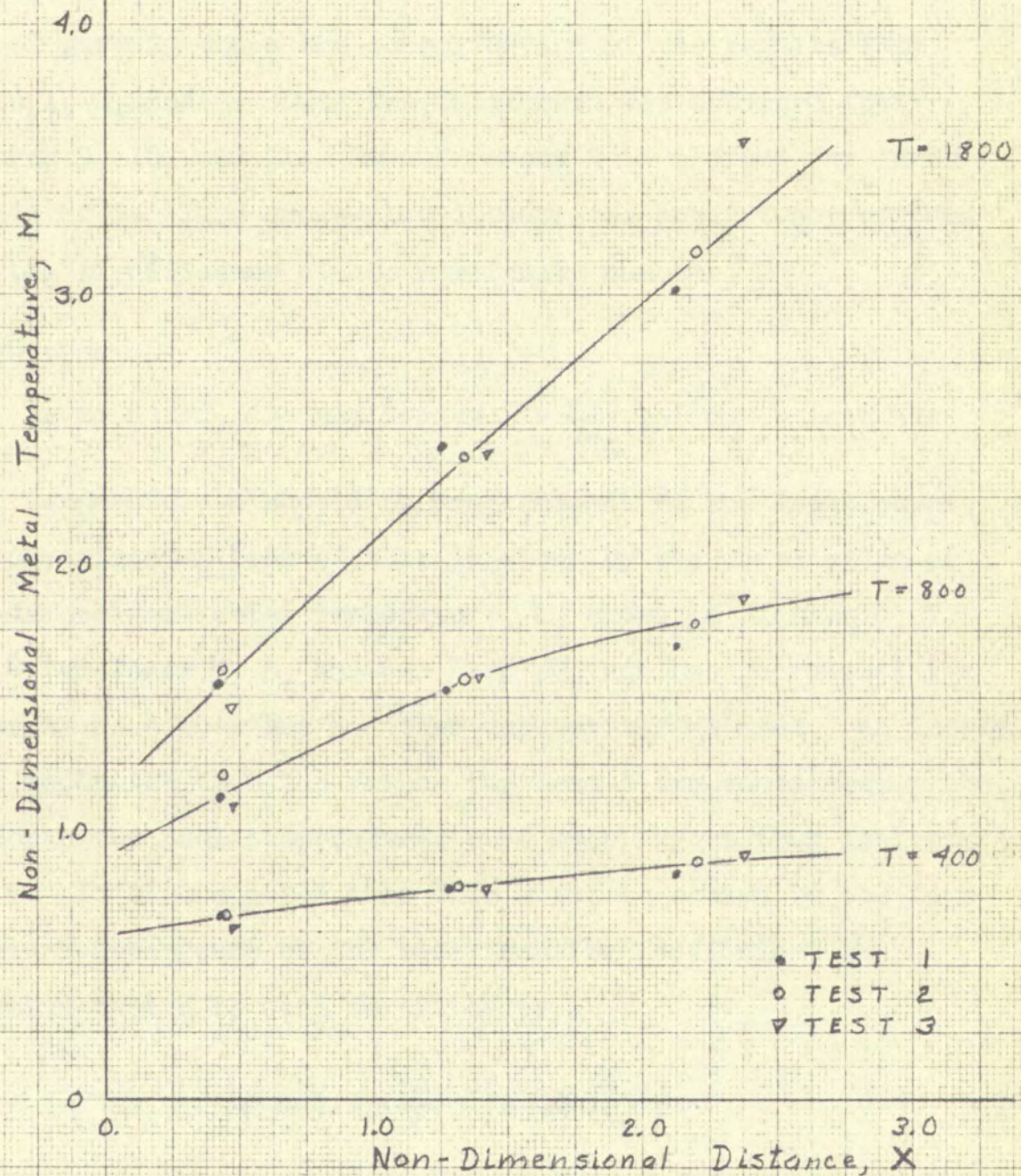

FIGURE 13 CROSS-PLOT OF RESULTS FROM TESTS 1, 2, 3

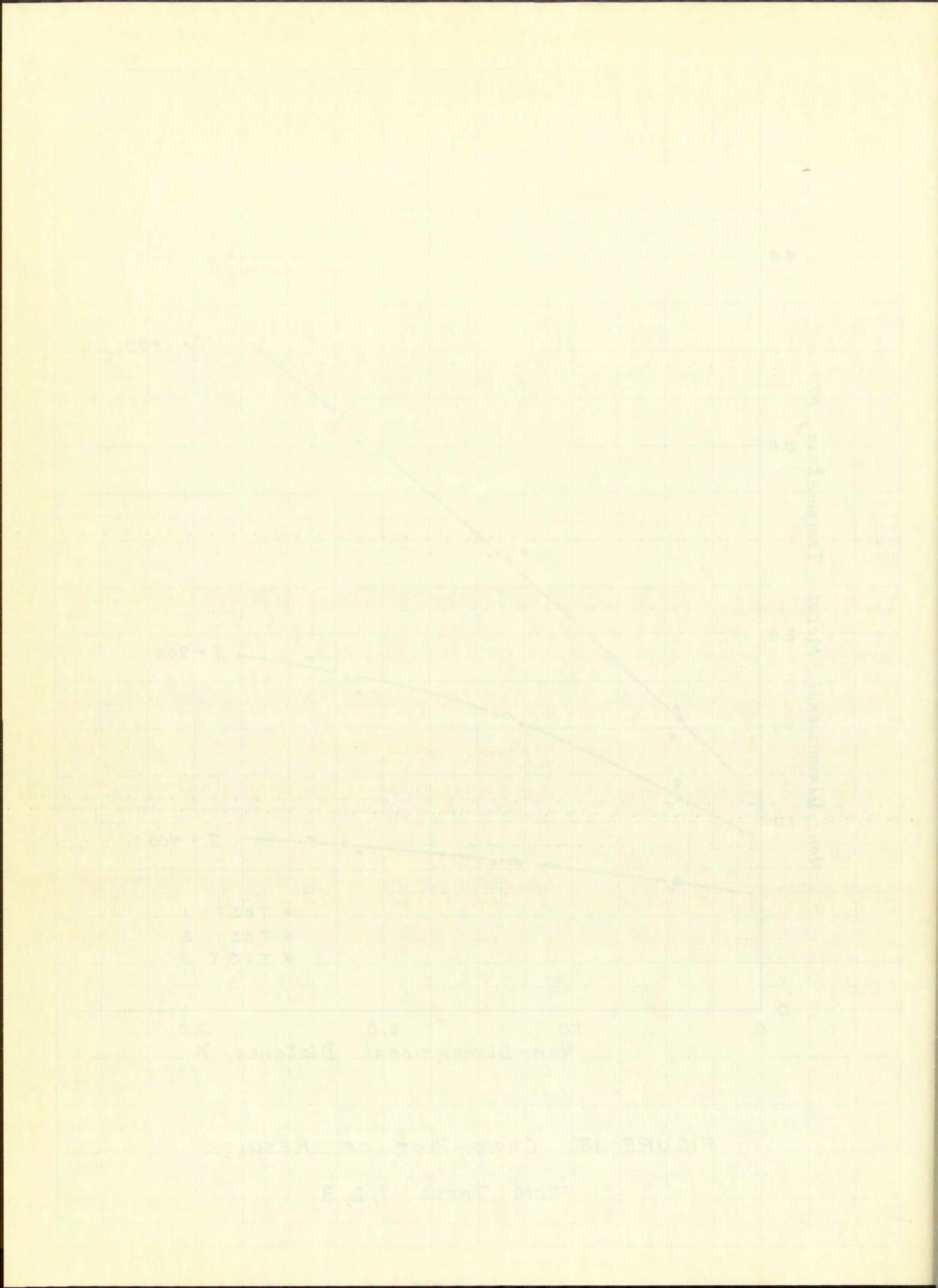

for X = 2.55 which corresponds to x = 72 inches for those tests. The theoretical curve for the same X is plotted with the experimental results.

Figure 13 shows the consolidation of the results from Tests 1, 2, and 3. Data for this graph was obtained from Figures 9, 10, and 11. Here M versus X is plotted for three values of T. This cross-plot illustrates consistency of data and the significance of the similarity numbers.

DISCUSSION

As expected, the similarity $M = \frac{mhp}{\Delta U_g}$ indicates that the real temperature m should be proportional to the input power. The experimental test of this is shown by the correlation of non-dimensional metal temperature, M, shown in Figures 6, 7, and 8 for Tests 4, 5, and 6. Here ΔU_g has been corrected for external heat loss but no other correction was made. An inspection indicates that the values for Test 5 are consistently low although the real temperatures were much higher than in Tests 4 and 6. It is suspected that this might be caused by the temperature dependence of the heat transfer coefficient h. Assuming that h is well described by

$$\frac{hD}{k} = 0.23\left(\frac{DG}{\mu}\right)^{0.8}\left(\frac{c_p\mu}{k}\right)^{0.4}, \qquad 29$$

the temperature dependence may be attributed to k and μ by

$$h \propto \frac{(k)^{0.6}}{(\mu)^{0.4}},$$

and

$$\frac{h_4}{h_5} = \left(\frac{\mu_5}{\mu_4}\right)^{0.4}\left(\frac{k_4}{k_5}\right)^{0.6} \quad . \qquad 32$$

The variables are evaluated as follows:

$\mu_4 = 0.021$ at 200°F

$\mu_5 = 0.029$ at 600°F

$k_4 = 0.0184$ at 200°F

$k_5 = 0.0260$ at 600°F

Substitutions of these values in equation 32 gives

$$h_4 = h_5(1.38)^{0.4}(0.707)^{0.6}$$

or

$$h_4 = 0.925\ h_5.$$

The dimensionless M is directly proportional to h. Therefore, a deviation of approximately 7-1/2% between the curves for Test 4 and Test 5 is explained by the temperature dependence of h. This is about the magnitude of the deviation in Figures 6, 7, and 8. Taking the above into account, the agreement between tests is sufficient to justify the method by which ΔU_g was corrected for external heat loss.

The principal results of the investigation are illustrated by Figures 9, 10, 11, and 12. The departure of the theoretical curves from the experimental curves is characterized by an

initial overstatement and a final understatement of temperatures. The cross-over occurs at a time corresponding to about half of the time required to reach equilibrium which is achieved in the same time for both. Considering that the numerical computation assumed fluid properties at a median temperature of 300°F, the comparison is good.

The consistency of data is partially shown by the agreement among tests in Figures 6, 7, and 8. A comprehensive demonstration of consistency is presented by the cross-plot in Figure 13. In non-dimensional terms, Figure 13 indicates that the similarity theory, experimental data and calculations are probably valid since the results are consistent and are comparable to the numerical solution.

CHAPTER 6

CONCLUSIONS AND RECOMMENDATIONS

The following conclusions can be drawn from this investigation:

1. Transient performance of a heat exchanger with an internal source can be correlated by use of the similarity numbers $M = \frac{mhp}{\Delta U_g}$, $F = \frac{fhp}{\Delta U_g}$, $X = \frac{fhp}{\Delta U_g}$,

   $T = \frac{thp}{c_f \gamma_f A_f}$, and $a = \frac{c_m \gamma_m A_m}{c_f \gamma_f A_f}$.

2. The use of an average temperature for fluid properties gives a numerical solution which overstates initial temperatures and understates final temperatures for the conditions of this investigation.
3. The assumption of constant fluid properties may lead to significant error when temperature changes are $400^{\circ}F$ or greater.
4. The analytical solution must be further simplified before it becomes useful as a design tool.

An analytical solution of this problem for design application has still not been achieved and it is recommended that further efforts be directed toward the simplification of the results obtained in this investigation. The approach to this problem might be the division of the problem into the special cases of small "a" and large "a," small "X" and large "X," etc.

It should be borne in mind, however, that the analytical solution may not represent the physical problem very closely unless temperature dependent effects are accounted for. This suggests that a more sophisticated numerical method might be more useful, but a digital computer should be used to reduce the labor.

Additional work on the thermal analog discussed here might be rewarding. The similarity numbers derived appears to be quite significant, and it is believed that the analog approach should give good results which would be valuable in design studies. Further analog results would also be of assistance in deriving, as well as verifying, new theoretical approaches.

Some refinements are recommended in the present apparatus. The starting point should be the development of a better method for installing thermocouples on the tube. A low-heat-capacity insulation around the heated tube would reduce external heat losses and improve the precision of the results. The possibility of measuring bulk coolant temperature at several points might also be investigated. A more stable power source and a larger air supply tank might contribute to slight improvements in data.

APPENDIX

LIST OF REFERENCES

(1) Schultz, M. A. Control of Nuclear Reactors and Power Plants, McGraw-Hill Book Co., New York, N.Y., 1955.

(2) Howard, R. C. Evaluation of the Nonlinear Kinetic Behavior of a Nuclear Power Reactor, Transactions of the ASME, 163-169, January 1956.

(3) Brown, Dale H. Transient Thermodynamics of Reactors and Process Apparatus, 2nd Nuclear Engineering and Science Conference, Philadelphia, 1957, ASME Paper No. 57-NESC-81.

(4) Bonilla, Charles F. The Importance of Dependable Approximation Methods in Nuclear Engineering, Journal of Engineering Education, 328-332, December 1954.

(5) Hellman, S. K., George Habetter, and Harold Babrov. Use of Numerical Analysis in the Transient Solution of Two-Dimensional Heat-Transfer Problem with Natural and Forced Convection, Transactions of the ASME, 1155-1161, August 1956.

(6) Dusinberre, G. M. Calculation of Transient Temperatures in Pipes and Heat Exchangers by Numerical Methods, Transactions of the ASME, 421-426, April 1954.

(7) Paynter, H. M. and Yasundo Takahashi. A New Method of Evaluating Dynamic Response of Counterflow and Parallel-Flow Heat Exchangers, Transactions of the ASME, 749-758, May 1956.

(8) Rizika, J. W. Thermal Lags in Flowing Systems Containing Heat Capacitors, Transactions of the ASME, 411-420, April 1954.

(9) Rizika, J. W. Thermal Lags in Flowing Incompressible Fluid Systems Containing Heat Capacitors, Transactions, of the ASME, 1407-1413, October 1956.

(10) Clark, J. A., V. S. Arpaci, and K. M. Treadwell. Dynamic Response of Heat Exchangers Having Internal Heat Sources-Part I, Transactions of the ASME, 612-624, April 1958.

(11) Clark, J. A. and V. S. Arpaci. Dynamic Response of Heat Exchangers Having Internal Heat Sources - Part II, Transactions of the ASME, 625-634, April 1958.

(12) Treadwell, K. M. Theoretical and Experimental Investigation of Fluid Temperature Response in Flowing Incompressible Fluid Systems with Internal Heat Generation. Unpublished SM thesis, Department of Mechanical Engineering, Massachusetts Institute of Technology, Cambridge, Mass., July 1955.

(13) Stuart, W. M. Thermal Response of Nuclear Reactor Coolants to Power Transients. Unpublished SB thesis, Department of Mechanical Engineering, Massachusetts Institute of Technology, Cambridge, Mass., May 1956.

(14) Bankston, Charles. A Numerical Solution of a Transient Heat Transfer Problem. Unpublished research, Department

of Mechanical Engineering, University of New Mexico, Albuquerque, N.M., February 1958.

(15) Bateman Manuscript Project. Table of Integral Transforms, Vol. 1, McGraw-Hill Book Co., New York, N.Y., 1954.

(16) Churchill, Ruel V. Modern Operational Mathematics in Engineering, 1st Ed., McGraw-Hill Book Co., New York, N.Y., 1944.

(17) Pipes, Lewis A. Applied Mathematics for Engineers and Physicists, 1st Ed., McGraw-Hill Book Co., New York, N.Y., 1946.

(18) Wheelon, Albert D. and John T. Robacker. Table of Integrals Involving Bessel Functions, The Ramo-Wooldridge Corporation, Los Angeles, Calif., 1954.

(19) Grace, H. P. and C. E. Lapple. Discharge Coefficients of Small-Diameter Orifices and Flow Nozzles, Transactions of the ASME, 639-647, July 1951.

(20) Summers, Thomas O., Department of Electrical Engineering, University of New Mexico, Albuquerque, N.M., (Private communication), 1958.

(21) Giedt, Warren H. Principles of Engineering Heat Transfer, D. Van Nostrand Co., Inc., Princeton, New Jersey, 1957.

TABLE 1

COMPARISON OF THERMOMETER IN SPECIAL WELL

AND TUBE THERMOCOUPLES

Test A - Comparison with iron-constantan thermocouple at x = 36 inches.

Date: 14 June 1958

Thermometer in well °F	Chromel-Alumel TC in well °F	Iron-Constantan TC on tube °F
equilibrium		
598	592	592
605	600	607
tube cooling		
	535	520
readings taken in succession	500	482
	230	225
	220	218
	213	210
	207	207

TABLE 1 (Continued)

COMPARISON OF THERMOMETER IN SPECIAL WELL

AND TUBE THERMOCOUPLES

Test B - Comparison with chromel-alumel thermocouple at x = 60 inches.

Date: 17 June 1958

Thermometer in well °F	Chromel-Alumel TC in well °F	Chromel-Alumel TC on tube °F
equilibrium		
640	642	662
640	642	662
tube cooling		
	337	322
readings taken in succession	303	294
	288	283
	278	275
	270	270
	262	259

TABLE 2

FACTOR K FOR CONVERTING OSCILLOGRAPH

TRACE DEFLECTION TO TEMPERATURE

Circuit	Factor K = °F/inch	Probable Error, °F (Assuming ± 1/64" reading accuracy)
Galv. No. 2 - T.C. at 1/2" or 6"	657	± 10
Galv. No. 3 - T.C. at 12"	577	± 9
Galv. No. 4 - T.C. at 36"	593	± 9
Galv. No. 5 - T.C. at 60"	1130	± 18
Galv. No. 6 - T.C. at 66" or 71-1/2"	1040	± 16
Galv. No. 10 with amplifier - Fluid Temp. Probe	235	± 4

TABLE 3

EXTERNAL HEAT LOSS MEASUREMENT

Test No. 1 Date: 17 June 1958

Input Power, watts/inch	Metal Temp. °F at x = 1/2"	Metal Temp. °F at x = 12"	Metal Temp. °F at x = 36"	Metal Temp. °F at x = 60"	Metal Temp. °F at x = 72-1/2"
0.69	56	88	92	90	43
1.47	118	175	178	178	91
3.10	189	287	303	305	157
4.89	272	404	427	440	228
7.59	357	523	550	575	317
10.0	430	625	657	708	398

Test No. 2 Date: 21 June 1958

Input Power, watts/inch	Metal Temp. at x = 6"(°F)	Metal Temp. at x = 12"(°F)	Metal Temp. at x = 36"(°F)	Metal Temp. at x = 60"(°F)	Metal Temp. at x = 66"(°F)
1.34	157	153	160	156	150
2.28	233	230	240	154	236
4.08	365	355	369	390	390
7.03	528	506	530	608	590

TABLE 4

RAW DATA - METAL TEMPERATURES

Flow Rate: 0.865 #/min
Power Input: 30.9 watts/in
Inlet Air Temp.: 82°F; Reference Junction (Room Temp.): 85°F

Date: 21 June 1958
Test No. 1

Time sec	Temp. (°F) at x = 6"			Temp. (°F) at x = 12"			Temp. (°F) at x = 36"			Temp. (°F) at x = 60"			Temp. (°F) at x = 66"		
	Run 1	Run 2	Avg	Run 1	Run 2	Avg	Run 1	Run 2	Avg	Run 1	Run 2	Avg	Run 1	Run 2	Avg
5	55	51	53	30	38	34	32	45	39	42	52	47	40	50	45
10	95	102	99	80	75	78	100	105	103	100	108	104	95	105	100
15	126	137	132	121	122	122	140	157	149	140	148	144	145	150	148
20	181	176	179	167	164	166	198	210	204	200	205	203	205	220	213
30	230	223	227	227	223	225	283	284	284	282	282	282	310	295	303
40	268	255	262	275	267	271	345	340	343	358	355	357	390	385	388
50	287	272	280	305	293	299	390	392	391	420	410	415	455	440	448
70	312	297	305	340	322	331	456	444	450	510	490	500	540	520	530
90	325	308	317	355	335	345	482	468	475	575	545	560	600	575	588
120	317	321	319	350	348	349	492	488	490	595	580	588	615	600	608
150	327	315	321	360	342	351	498	490	494	608	580	594	620	595	608
measured	306	335	321	334	329	332	472	473	473	598	585	592	610	588	599

TABLE 4 (Continued)

RAW DATA - METAL TEMPERATURES

Flow Rate: 0.708 #/min
Power Input: 30.9 watts/in
Inlet Air Temp.: 85°F; Reference Junction (Room Temp.): 86°F

Date: 21 June 1958

Test No. 2

Time sec	Metal Temp. (°F) at x = 6" Run 1	Run 2	Avg	Metal Temp. (°F) at x = 12" Run 1	Run 2	Avg	Metal Temp. (°F) at x = 36" Run 1	Run 2	Avg	Metal Temp. (°F) at x = 60" Run 1	Run 2	Avg	Metal Temp. (°F) at x = 66" Run 1	Run 2	Avg
5	-	40	-	38	28	32	44	40	42	50	45	48	55	40	48
10	-	82	-	85	78	81	88	97	93	100	90	95	105	95	100
15	-	127	-	135	130	133	148	160	154	165	155	160	170	160	165
20	-	181	-	177	165	171	227	210	219	220	205	213	230	215	223
30	-	243	-	242	237	240	313	298	306	310	295	303	335	305	320
40	-	275	-	288	282	285	387	375	381	395	370	383	415	390	403
50	-	296	-	326	306	317	438	422	430	475	445	460	480	450	465
70	-	323	-	362	346	354	502	480	491	578	540	559	575	540	558
90	-	345	-	378	358	368	532	520	526	630	605	618	620	590	605
120	-	332	-	378	380	279	532	542	540	670	695	683	670	630	650
150	-	320	-	382	372	279	552	548	550	675	725	700	665	640	653
measured	347	351	349	349	389	269	531	543	537	667	685	676	667	685	676

TABLE 4 (Continued)

RAW DATA - METAL TEMPERATURES

Flow Rate: 0.50 #/min
Power Input: 30.9 watts/in
Inlet Air Temp.: 87°F; Reference Junction (Room Temp.): 86°F

Date: 21 June 1958

Test No. 3

Time Sec	Metal Temp. (°F) x = 6" Run 1	Run 2	Avg	Metal Temp. (°F) x = 12" Run 1	Run 2	Avg	Metal Temp. (°F) x = 36" Run 1	Run 2	Avg	Metal Temp. (°F) x = 60" Run 1	Run 2	Avg	Metal Temp. (°F) x = 66" Run 1	Run 2	Avg
5	35	40	38	37	33	35	48	45	47	40	50	45	45	45	45
10	68	82	75	74	80	77	100	102	101	85	100	93	85	105	95
15	102	120	111	122	124	123	162	168	165	145	160	153	155	150	153
20	125	153	139	160	169	165	208	218	213	190	212	201	200	215	208
30	183	198	191	241	234	238	318	304	311	295	300	298	305	305	305
40	223	235	229	302	285	294	405	382	394	390	380	385	395	385	390
50	246	263	255	341	323	332	470	445	458	485	465	475	485	470	478
70	274	302	288	400	383	392	553	537	545	620	615	618	595	600	598
90	294	321	308	427	412	420	605	592	599	710	700	705	685	675	680
120	300	335	318	445	438	442	643	627	635	775	735	755	735	740	738
150	308	304	306	448	438	443	663	640	652	825	770	797	775	745	760
measured	445	450	448	477	478	478	647	655	651	821	830	826	802	795	799

TABLE 4 (Continued)

RAW DATA - METAL TEMPERATURES

Flow Rate: 0.865 #/min
Power Input: 13.9 watts/in
Inlet Air Temp.: 85°F; Reference Junction (Room Temp.): 88°F

Date: 23 June 1958

Test No. 4

Time sec	Metal Temp. (°F) x = 6" Run 1	Run 2	Avg	Metal Temp. (°F) x = 12" Run 1	Run 2	Avg	Metal Temp. (°F) x = 36" Run 1	Run 2	Avg	Metal Temp. (°F) x = 60" Run 1	Run 2	Avg	Metal Temp. (°F) x = 66" Run 1	Run 2	Avg
5	20	15	18	24	20	22	20	23	22	32	30	31	25	30	28
10	42	25	31	42	35	39	45	46	46	52	45	49	53	55	54
15	56	35	47	61	56	59	71	73	72	73	60	67	80	82	81
20	70	47	59	82	77	80	96	96	96	93	92	93	110	110	110
30	90	56	73	112	102	107	137	133	135	142	123	133	158	147	153
40	106	67	87	130	123	127	165	165	165	168	159	164	197	200	199
50	111	68	90	142	133	138	188	190	189	185	182	184	232	220	226
70	116	75	96	155	138	147	213	206	210	220	208	214	268	258	253
90	122	80	101	156	145	151	218	216	217	235	223	229	278	280	279
120	122	80	101	157	146	153	230	228	229	248	242	245	302	282	292
150	125	-	-	165	-	-	234	-	-	260	-	-	312	-	-
measured	140	135	138	155	150	153	225	226	226	284	276	280	298	294	296

TABLE 4 (Continued)

RAW DATA - METAL TEMPERATURES

Flow Rate: 0.865 #/min
Power Input: 41.6 watts/in
Inlet Air Temp.: 91°F; Reference Junction (Room temp.): 90°F

Date: 23 June 1958

Test No. 5

Time sec	Metal Temp. (°F) x = 6" Run 1	Run 2	Avg	Metal Temp. (°F) x = 12" Run 1	Run 2	Avg	Metal Temp. (°F) x = 36" Run 1	Run 2	Avg	Metal Temp. (°F) x = 60" Run 1	Run 2	Avg	Metal Temp. (°F) x = 66" Run 1	Run 2	Avg
5	37	41	39	40	46	43	57	61	59	32	42	37	50	52	51
10	93	87	90	98	93	96	132	131	132	110	112	111	128	125	127
15	136	126	131	150	148	149	200	202	201	180	175	178	205	193	199
20	173	158	166	203	194	199	267	266	267	243	238	241	268	265	267
30	220	207	214	274	268	271	375	370	373	364	362	363	398	382	390
40	250	237	244	322	322	322	446	444	445	470	463	467	495	478	487
50	270	257	264	356	354	355	502	495	499	455	552	554	568	550	559
70	293	266	280	392	386	389	566	551	559	655	655	655	662	638	650
90	305	261	283	412	402	407	598	581	590	710	703	707	712	690	701
120	308	272	290	418	406	412	615	597	606	740	732	735	732	712	722
150	308	273	290	422	-	-	615	-	-	757	-	-	740	-	-
measured	402	402	402	440	447	444	618	610	614	795	780	788	785	781	783

TABLE 4 (Continued)

RAW DATA - METAL TEMPERATURES

Flow Rate: 0.865 #/min
Power Input: 39.9 watts/in
Inlet Air Temp.: 97°F; Reference Junction (Room Temp.): 92°F

Date: 23 June 1958

Test No. 6

Time Sec	Metal Temp. (°F) x = 6" Run 1	Run 2	Avg	Metal Temp. (°F) x = 12" Run 1	Run 2	Avg	Metal Temp. (°F) x = 36" Run 1	Run 2	Avg	Metal Temp. (°F) x = 60" Run 1	Run 2	Avg	Metal Temp. (°F) x = 66" Run 1	Run 2	Avg
5	42	33	38	31	30	31	47	42	45	25	32	29	45	42	44
10	80	73	77	67	70	69	97	97	97	75	90	82	95	93	94
15	120	121	121	111	110	111	157	150	154	128	148	138	147	156	152
20	152	146	149	148	145	147	210	202	206	197	193	195	212	202	207
30	195	188	192	200	200	200	282	276	279	266	275	270	300	294	297
40	218	222	220	230	239	235	335	334	335	338	350	344	365	362	364
50	237	237	237	257	264	261	382	376	379	402	396	399	432	412	422
70	251	256	254	286	293	290	429	426	428	473	485	479	512	493	503
90	252	266	259	298	307	303	445	460	448	508	538	523	542	550	546
120	256	268	262	300	313	307	453	466	460	518	563	541	542	568	555
150	-	-	-	-	-	-	-	-	-	-	-	-	-	-	-
measured	310	317	315	345	350	348	477	482	480	610	613	612	620	621	621

TABLE 5

RAW DATA - FLUID EXIT TEMPERATURE

Refer to Table 4 for Test Conditions

Time sec	Test No. 1 Run 1	Run 2	Avg	Test No. 2 Run 1	Run 2	Avg	Test No. 3 Run 1	Run 2	Avg
5	55	50	53	39	48	44	50	46	48
10	85	102	94	104	103	104	105	103	104
15	145	148	147	160	155	158	152	168	160
20	187	189	188	206	201	204	200	200	200
30	266	266	266	288	280	284	294	280	287
40	327	322	325	347	345	346	372	355	364
50	373	363	368	402	392	397	440	418	429
70	438	418	428	468	462	465	539	507	523
90	475	453	465	507	505	506	591	564	578
120	490	480	485	542	537	540	642	623	633
150	500	490	495	555	552	554	668	655	662
measured	503	510	507	568	569	569	690	685	688

TABIE 5 (Continued)

RAW DATA - FLUID EXIT TEMPERATURE

Refer to Table 4 for Test Conditions

Time sec	Test No. 4			Test No. 5			Test No. 6		
	Run 1	Run 2	Avg	Run 1	Run 2	Avg	Run 1	Run 2	Avg
5	25	25	25	72	73	73	58	56	57
10	47	48	48	143	144	144	120	117	119
15	68	69	69	206	206	206	172	172	172
20	80	89	84	265	264	265	218	222	220
30	122	126	124	362	360	361	287	290	289
40	148	156	152	432	437	435	350	353	352
50	168	175	172	488	488	488	396	402	399
70	194	196	195	552	564	558	455	466	461
90	210	212	211	592	600	596	488	521	505
120	224	226	225	618	632	625	-	-	-
150	228	-	-	632	642	635	-	-	-
measured	240	241	241	660	640	650	518	518	507

TABLE 6

RESULTS - METAL TEMPERATURES

Test No. 1 and 6 consolidated

	X = 0.425 x = 12"			X = 1.275 x = 36"			X = 2.125 x = 60"		
Dimensionless Time, T	Smoothed Temp. (°F)	External Heat Loss (watts/in)	Dimensionless Temp., M	Smoothed Temp. (°F)	External Heat Loss (watts/in)	Dimensionless Temp., M	Smoothed Temp. (°F)	External Heat Loss (watts/in)	Dimensionless Temp., M
110	36	0.2	0.156	40	0.3	0.174	43	0.3	0.187
220	81	0.6	0.356	90	0.7	0.396	98	0.7	0.432
440	161	1.4	0.725	189	1.7	0.861	210	1.9	0.963
880	244	2.4	1.14	313	3.2	1.51	368	4.0	1.82
1545	312	3.2	1.50	442	5.3	2.38	511	6.7	2.81
1990	326	3.4	1.57	466	5.8	2.47	548	7.5	3.11
2650	334	3.5	1.62	490	6.2	2.64	585	8.3	3.44
3310	338	3.6	1.65	495	6.3	2.67	594	8.5	3.53

TABLE 6 (Continued)

RESULTS - METAL TEMPERATURES

Test No. 2

	X = 0.440 x = 12"			X = 1.32 x = 36"			X = 2.20 x = 60"		
Non-Dimensional Time, T	Smoothed Temp., °F	External Heat Loss, (watts/in)	Non-Dimensional Temp., M	Smoothed Temp., °F	External Heat Loss, (watts/in)	Non-Dimensional Temp., M	Smoothed Temp., °F	External Heat Loss, (watts/in)	Non-Dimensional Temp., M
94	35	0.2	0.13	41	0.3	0.15	47	0.3	0.18
187	82	0.6	0.31	91	0.7	0.34	99	0.7	0.37
374	180	1.6	0.70	204	1.9	0.80	220	2.0	0.87
748	287	2.9	1.17	353	3.9	1.48	394	4.5	1.70
1310	353	3.8	1.47	467	5.8	2.22	550	7.5	2.68
1680	370	4.1	1.57	500	6.4	2.33	660	8.8	3.12
2240	380	4.2	1.62	523	6.9	2.48	628	9.4	3.33
2800	382	4.2	1.63	538	7.3	2.60	645	9.8	3.48

TABLE 6 (Continued)

RESULTS - METAL TEMPERATURES

Test No. 3

	X = 0.474 x = 12"			X = 1.42 x = 36"			X = 2.37 x = 60"		
Non-Dimensional Time, T	Smoothed Temp., °F	External Heat Loss,(watts/in)	Non-Dimensional Temp., M	Smoothed Temp., °F	External Heat Loss,(watts/in)	Non-Dimensional Temp., M	Smoothed Temp., °F	External Heat Loss,(watts/in)	Non-Dimensional Temp., M
71	37	0.2	0.10	40	0.3	0.11	44	0.3	0.13
142	77	0.5	0.22	88	0.6	0.25	98	0.7	0.28
284	157	1.3	0.46	188	1.6	0.56	210	1.9	0.63
568	269	2.6	0.82	342	3.7	1.08	387	4.3	1.26
993	360	3.9	1.15	508	6.6	1.80	600	8.7	2.34
1280	403	4.6	1.33	576	8.1	2.18	678	10.7	2.91
1700	423	4.9	1.41	617	9.1	2.45	730	13.0	3.52
2130	432	5.1	1.45	645	9.8	2.44	767	13.5	3.82

TABLE 6 (Continued)

RESULTS - METAL TEMPERATURES

Test No. 4

Dimensionless Time, T	X = 0.425 x = 12"			X = 1.275 x = 36"			X = 2.125 x = 60"		
	Smoothed Temp. (°F)	External Heat Loss (watts/in)	Dimensionless Temp., M	Smoothed Temp. (°F)	External Heat Loss (watts/in)	Dimensionless Temp., M	Smoothed Temp. (°F)	External Heat Loss (watts/in)	Dimensionless Temp., M
110	20	0.1	0.19	25	0.1	0.24	30	0.2	0.29
220	36	0.2	0.35	46	0.3	0.45	51	0.4	0.68
440	70	0.5	0.70	89	0.6	0.89	105	0.7	1.06
880	112	0.8	1.13	156	1.3	1.64	189	1.7	2.08
1545	140	1.2	1.46	204	1.8	2.24	252	2.4	2.91
1990	150	1.2	1.57	219	2.0	2.45	270	2.6	3.18
2650	153	1.3	1.61	229	2.1	2.58	282	2.8	3.38
3310	154	1.3	1.62	235	2.2	2.67	287	2.9	3.47

TABLE 6 (Continued)

RESULTS - METAL TEMPERATURES

Test No. 5

	X = 0.425 x = 12"			X = 1.275 x = 36"			X = 2.125 x = 60"		
Dimensionless Time, T	Smoothed Temp., °F	External Heat Loss (watts/in)	Dimensionless Temp., M	Smoothed Temp., (°F)	External Heat Loss (watts/in)	Dimensionless Temp., M	Smoothed Temp. (°F)	External Heat Loss, (watts/in)	Dimensionless Temp., M
110	42	0.3	0.14	45	0.3	0.15	48	0.3	0.15
220	97	0.7	0.32	119	0.9	0.39	130	1.1	0.43
440	188	1.6	0.63	229	2.2	0.77	255	2.5	0.87
880	318	3.3	1.10	420	4.9	1.52	472	5.9	1.76
1545	388	4.4	1.39	535	7.2	2.07	635	9.5	2.63
1990	407	4.7	1.47	575	8.1	2.28	696	10.8	3.00
2650	415	4.8	1.50	593	8.5	2.38	715	12.0	3.21
3310	421	4.9	1.53	606	8.8	2.45	732	12.5	3.35

TABLE 7

RESULTS - FLUID TEMPERATURES

Average data from Test 1 and 6

Dimensionless Time, T	Averaged Temp. (^{o}F)	External Heat Loss (watts/in)	Dimensionless Temp., F
110	55	0.3	0.238
220	107	0.8	0.473
330	159	1.3	0.715
440	204	2.0	0.94
660	278	3.0	1.32
880	339	4.3	1.69
1100	384	5.4	2.00
1540	445	7.0	2.50
1980	485	8.0	2.82
2640	508	8.8	3.05
measured	513	9.0	3.11

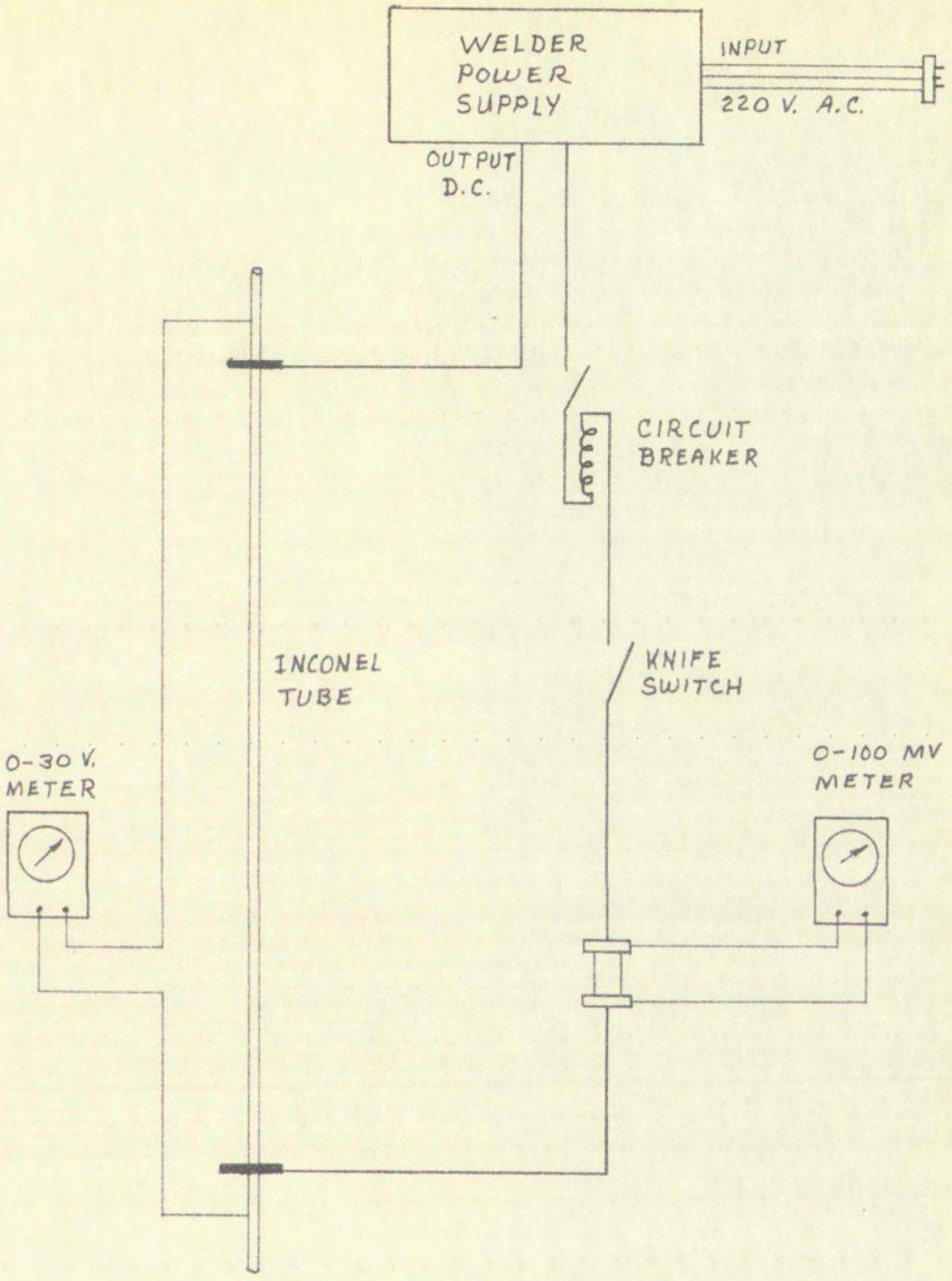

FIGURE 14 ELECTRICAL POWER CIRCUIT

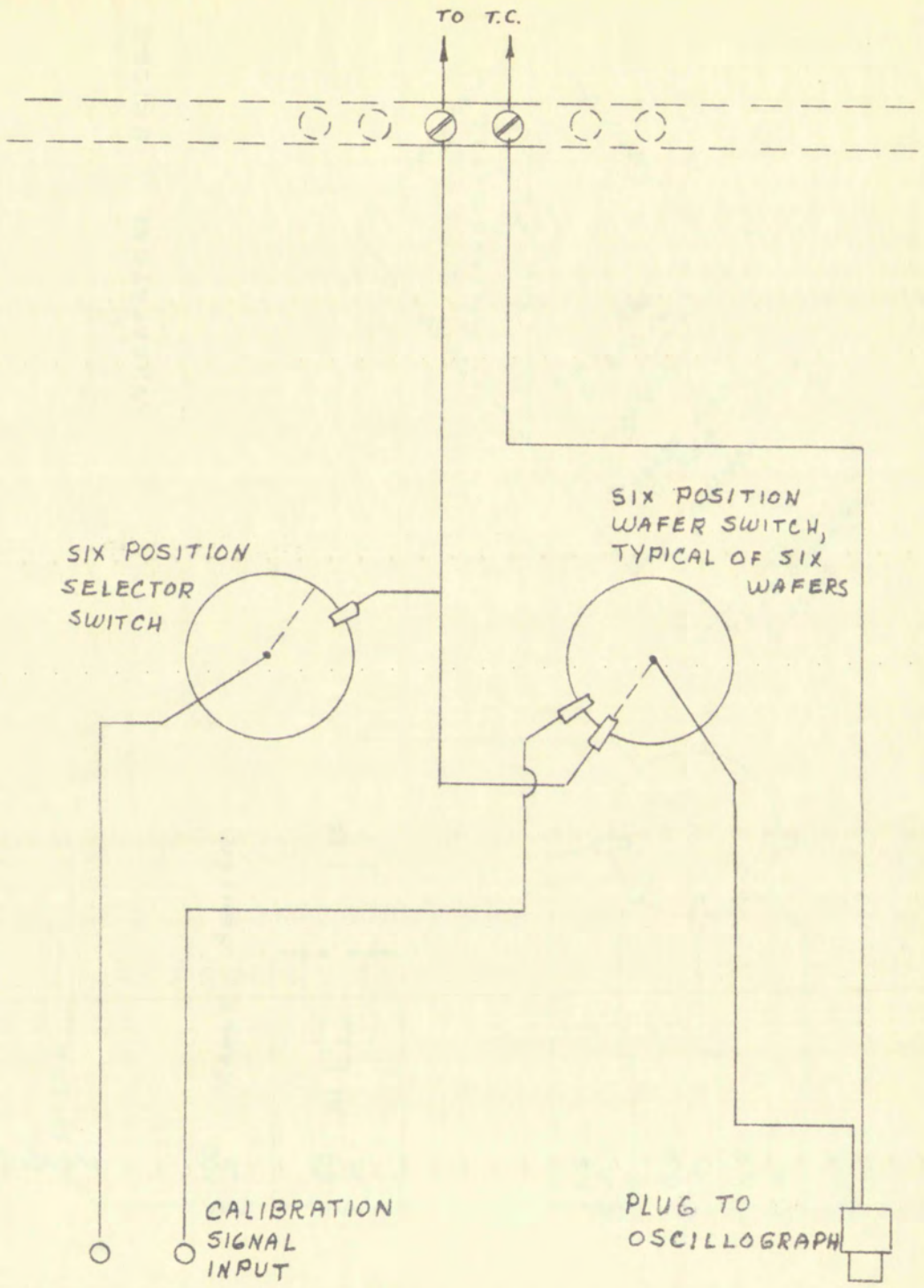

FIGURE 15 TYPICAL PORTION OF T. C. SWITCHING CIRCUIT

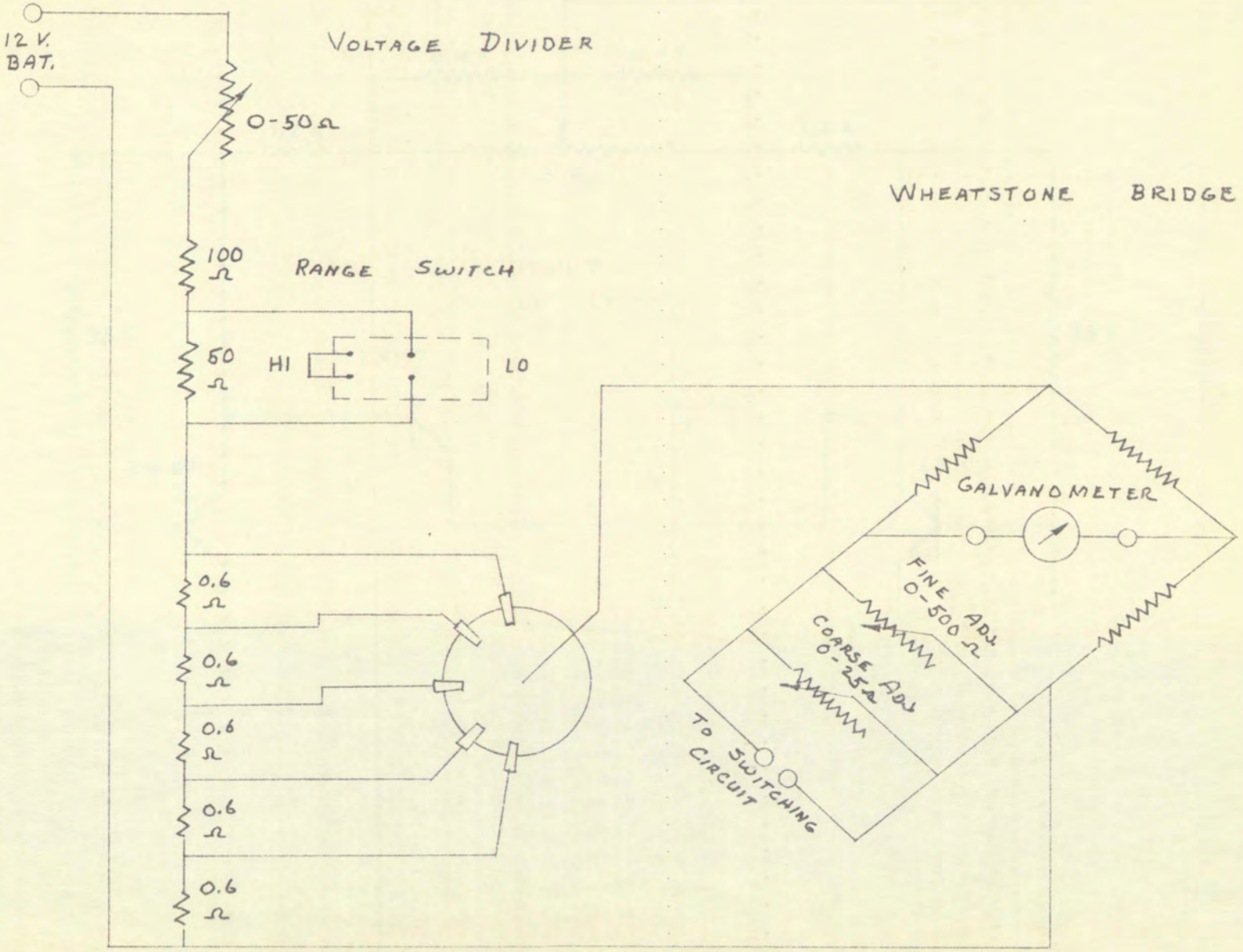

FIGURE 16 CALIBRATION CIRCUIT SCHEMATIC

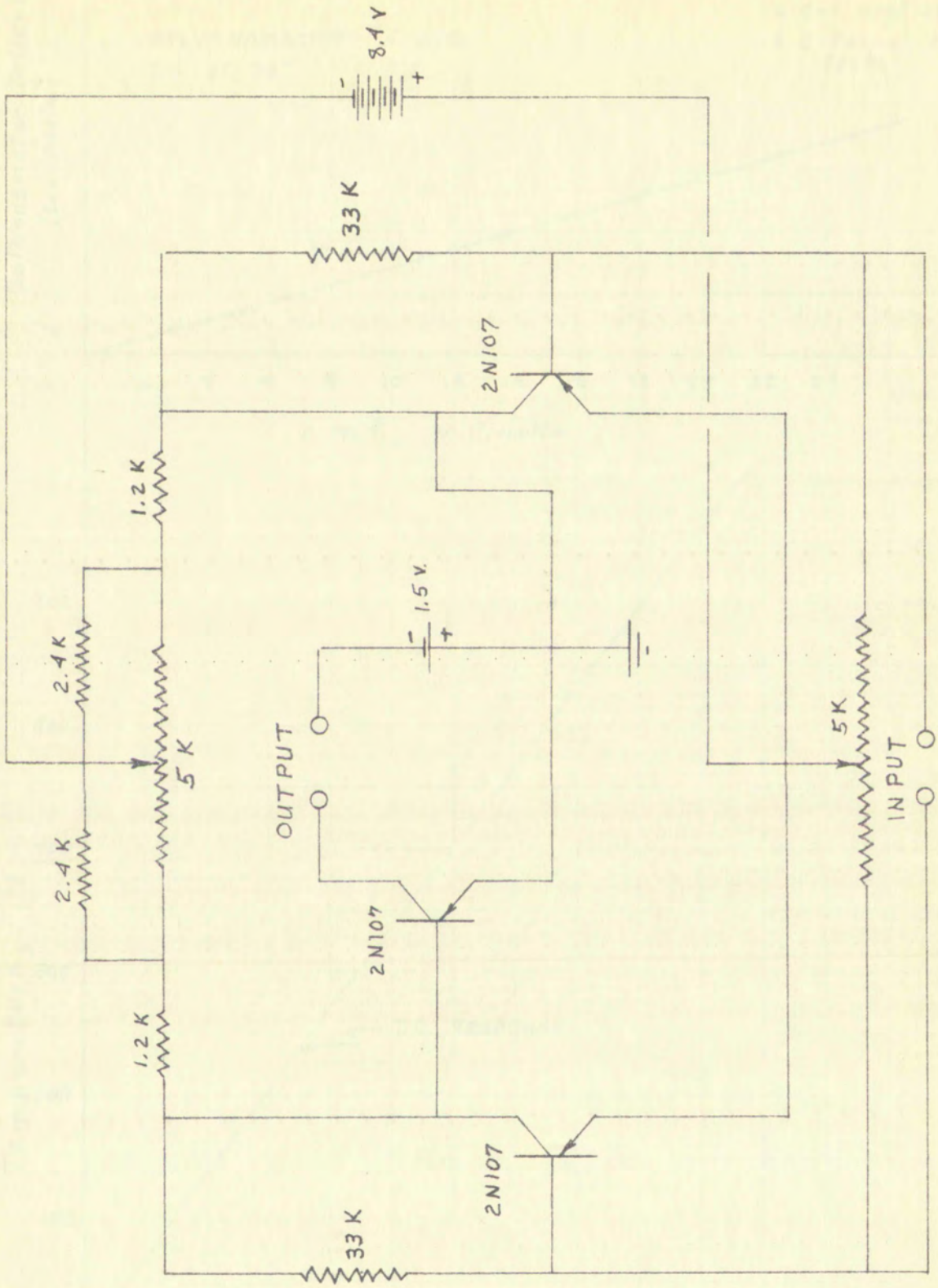

FIGURE 17 THERMOCOUPLE CURRENT AMPLIFIER

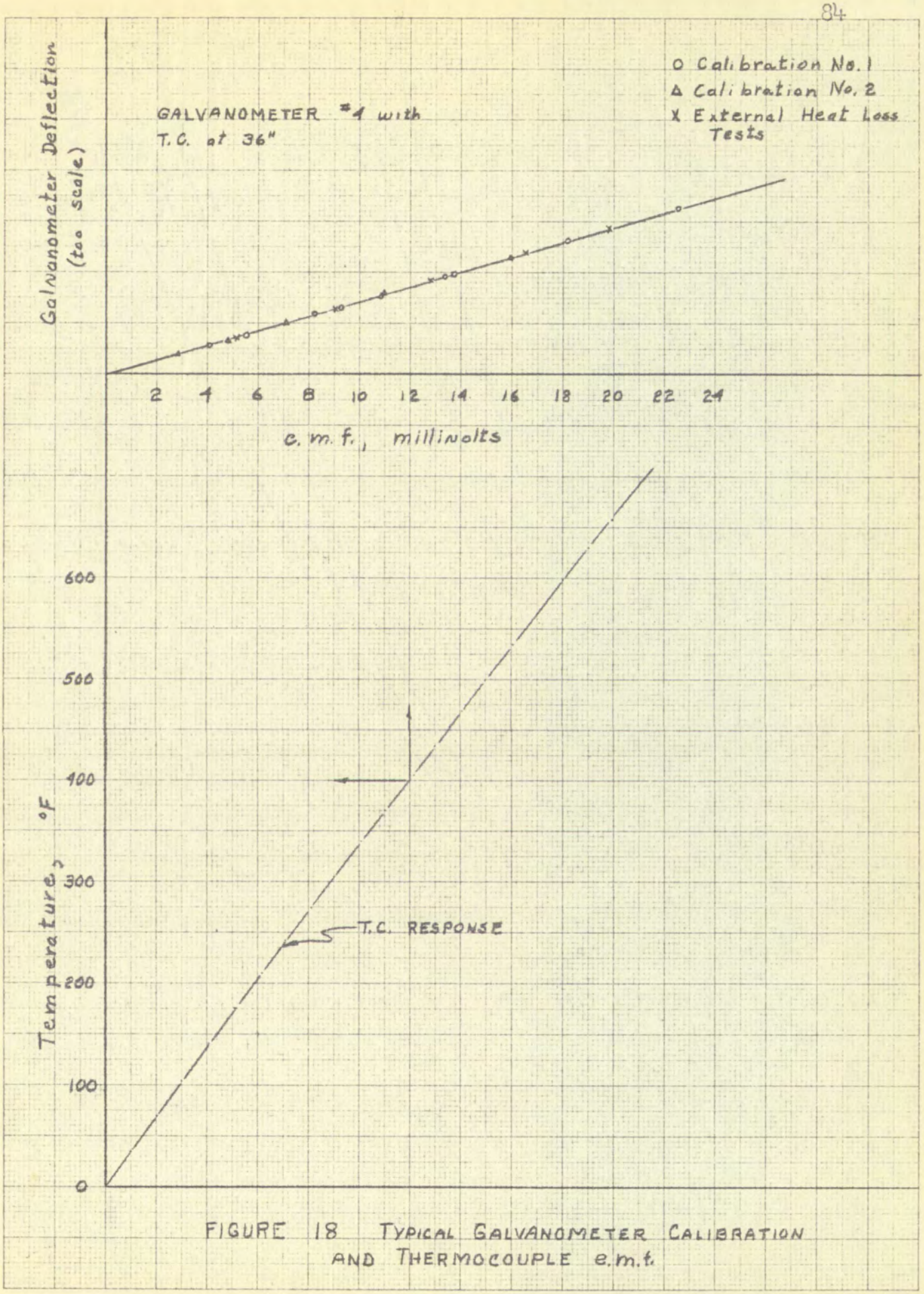

FIGURE 18 TYPICAL GALVANOMETER CALIBRATION AND THERMOCOUPLE e.m.f.

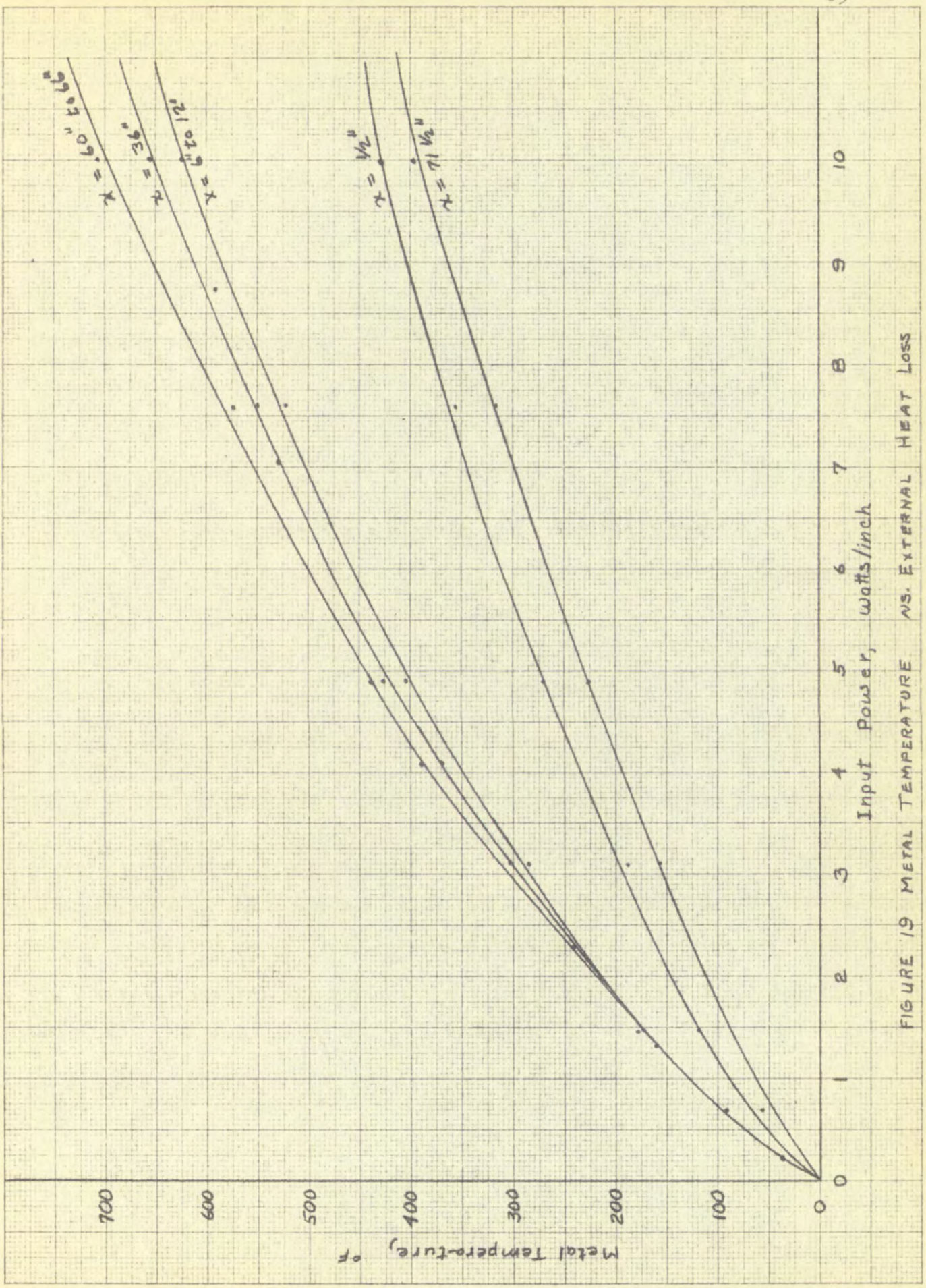

FIGURE 19 METAL TEMPERATURE VS. EXTERNAL HEAT LOSS

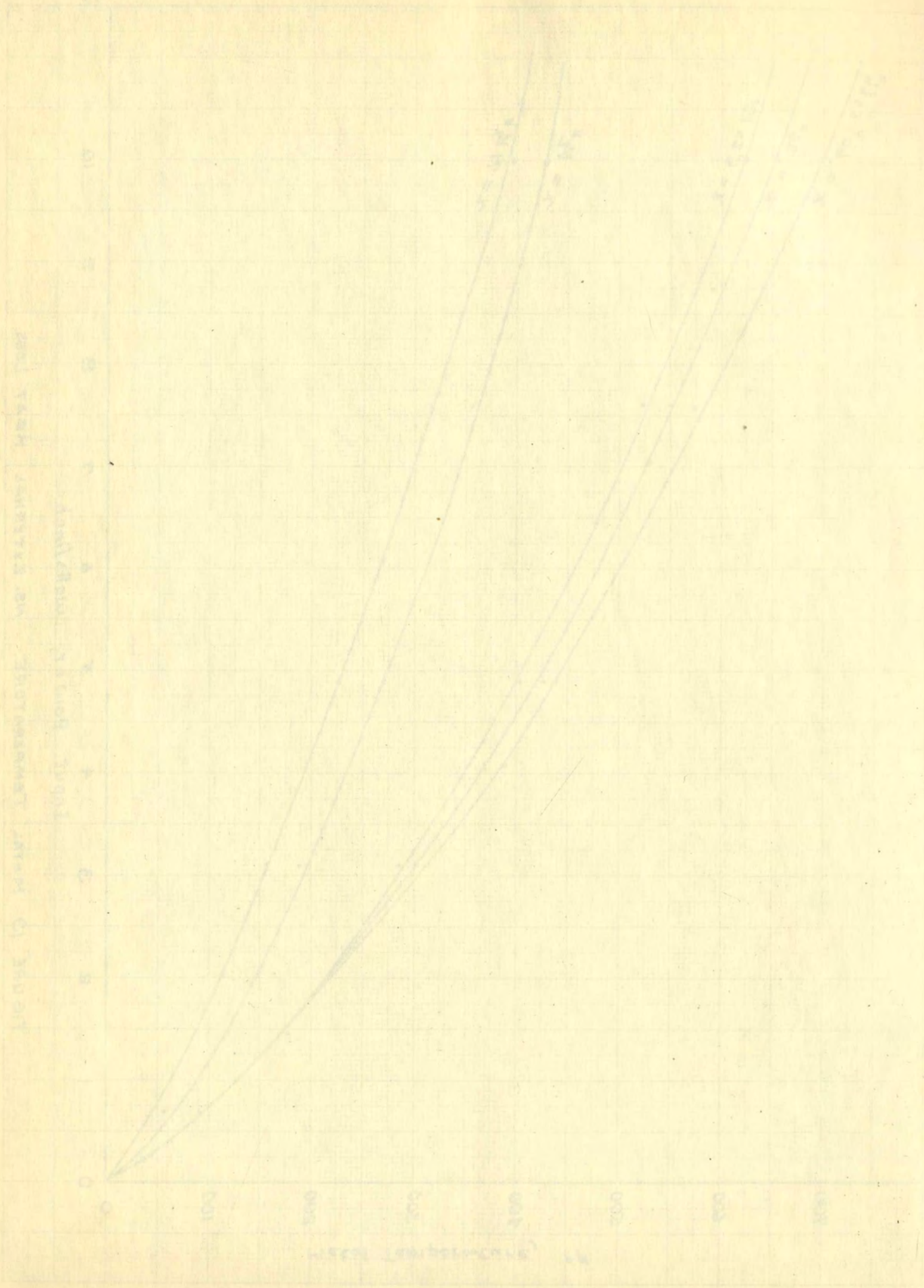

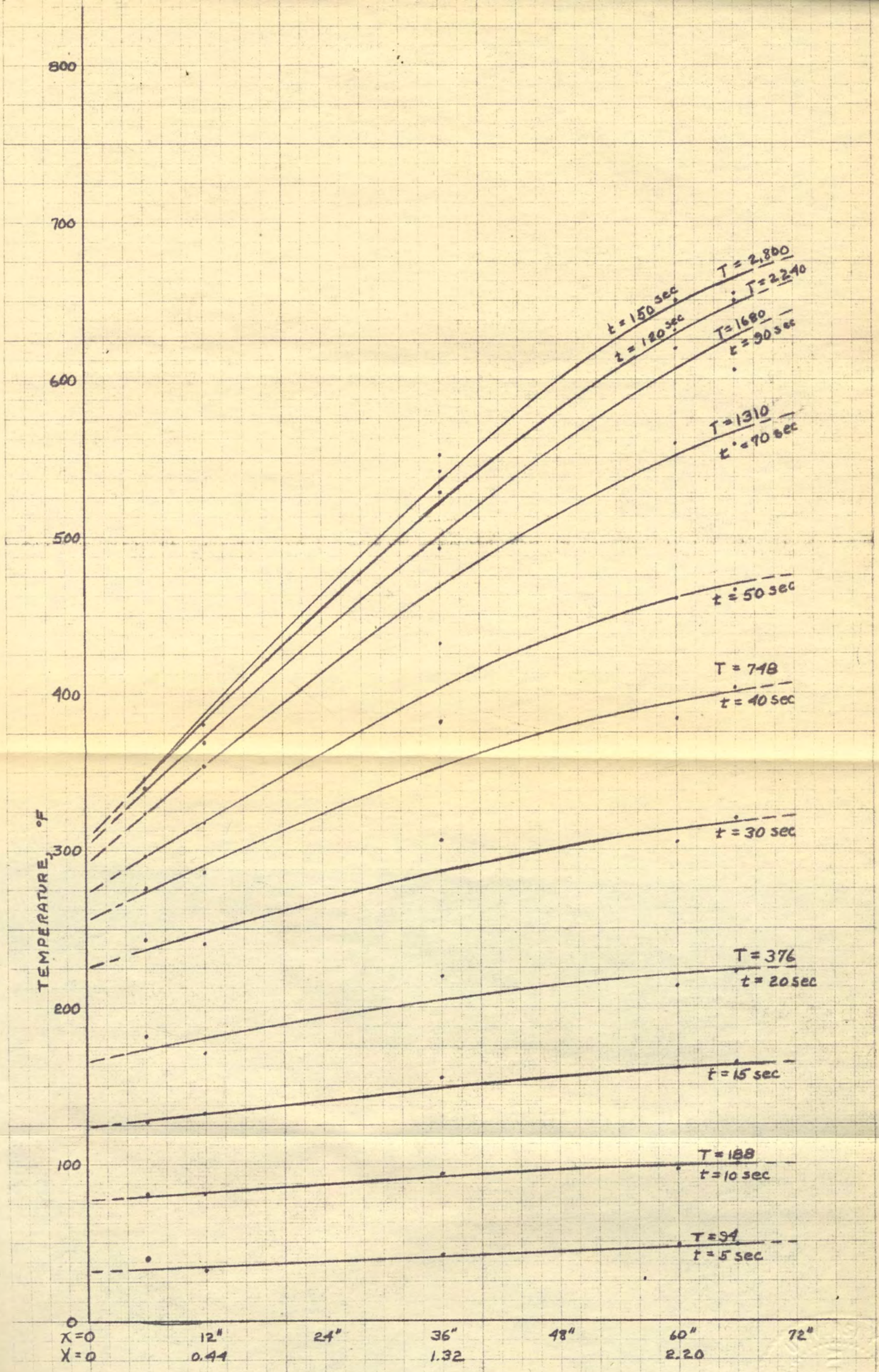

FIGURE 20 DATA SMOOTHING FOR TEST 2

IMPORTANT!

Special care should be taken to prevent loss or damage of this volume. If lost or damaged, it must be paid for at the current rate of typing.

Date Due			
	PRINTED	IN U. S. A.	